Title
INFRARED-ULTRAVIOLET DOUBLE RESONANCE STUDIES OF BENZENE MOLECULES IN A SUPERSONIC BEAM

Authors
Page, R.H.
Shen, Y.R.
Lee, Y.T.

Publication Date
1987-07-01

LBL-23769
Preprint

Lawrence Berkeley Laboratory
UNIVERSITY OF CALIFORNIA

Materials & Chemical Sciences Division

Submitted to Journal of Chemical Physics

Infrared-Ultraviolet Double Resonance Studies of Benzene Molecules in a Supersonic Beam

R.H. Page, Y.R. Shen, and Y.T. Lee

July 1987

Prepared for the U.S. Department of Energy under Contract DE-AC03-76SF00098

Submitted to Journal of Chemical Physics

INFRARED-ULTRAVIOLET DOUBLE RESONANCE STUDIES OF BENZENE MOLECULES IN A SUPERSONIC BEAM

Ralph H. Page,*(a) Y. R. Shen,* and Y. T. Lee†
Materials and Chemical Sciences Divison
Lawrence Berkeley Laboratory
University of California
Berkeley, California 94720
USA

ABSTRACT

We have used IR excitation to selectively create populations in admixtures of the zeroth-order states comprising the ~ 3000 cm^{-1} "C-H stretching Fermi triad" of benzene. UV spectra of the 260 nm $\tilde{A}$ ($^1B_{2u}$) ← $\tilde{X}$ ($^1A_{1g}$) transition in the IR-excited molecules show several new bands, which we have assigned. Final states in the UV transitions are some vibrational levels which have not been detected before, allowing us to find several excited-state vibrational frequencies. We have determined $\nu_3' = 1327 \pm 3$ cm^{-1}, $\nu_{19}' = 1405 \pm 3$ cm^{-1}, and $\nu_{20}' = 3084 \pm 5$ cm^{-1}. Also, vibrational structure which was unresolved in IR spectra of the "Fermi triad" was resolved in the UV double resonance spectra, confirming that the C-H stretching admixture is really a tetrad. The 3048, 3079, and 3101 cm^{-1} states had formerly been given the labels ν_{20}'', $\nu_8'' + \nu_{19}''$, and $\nu_1'' + \nu_6'' + \nu_{19}''$, respectively. Actually, the middle level most nearly resembles $\nu_1'' + \nu_6'' + \nu_{19}''$, and the 3101 cm^{-1} level is strongly mixed with $\nu_3'' + \nu_6'' + \nu_{15}''$.

As predicted by molecular orbital theory, excited-state C-H bending and stretching frequencies are not very different from those in the

ground state. Furthermore, we suggest that the four C-H stretching frequencies increase uniformly by ~20 cm^{-1} in the excited state; re-examination of the Atkinson and Parmenter 260 nm $\tilde{A} \leftarrow \tilde{X}$ spectrum leads us to reassign ν_2' from 3130 to ~3093 cm^{-1}, which is 19 cm^{-1} above ν_2''.

There is a Fermi resonance between the $\nu_6' + \nu_{20}'$ level and another level ~13 cm^{-1} lower in energy; the strength of the perturbation is ~18 cm^{-1}. Possibilities for the perturbing vibrational state are $\nu_6' + \nu_8' + \nu_{14}'$ and $\nu_6' + \nu_{13}'$.

PACS numbers-- 33.10.Gx 33.20.Lg 33.20.Ea 33.40.Ta

I. INTRODUCTION

The use of digital computers to perform ab initio calculations of intramolecular potentials, and to refine empirical force fields, has facilitated the theoretical modeling of molecules of ever-increasing size. In fact, the status quo is such that even the 12-atom benzene molecule, C_6H_6, has recently been the subject of detailed ab initio[1,2] and empirical[3-9] calculations. This is extremely significant because benzene is a textbook[10] "intermediate size" molecule and evidences many of the phenomena exhibited in other intermediate size molecules such as Fermi resonance, vibration-rotation coupling, and radiationless transitions. Its high degree of symmetry makes possible a reduction in the number of independent force constants used to parameterize its potential. The symmetry also forbids the appearance of some vibrational modes in the infrared absorption or Raman spectra, and guarantees that no mode can appear in both. This simplifies the spectra and allows clear interpretations and assignments of the observed modes.

Accordingly, the work on benzene has been quite extensive. In 1934 Wilson[11] calculated the normal coordinates and correctly assigned most of the modes observed in the infrared and Raman spectra. His system of numbering the modes, used in this article, is firmly entrenched in the literature, but is unfortunately different from the logical system of Herzberg.[12] The study of slightly altered (e.g. deuterated, $C_6H_nD_{6-n}$) benzene molecules, which have predictably perturbed normal modes and frequencies, has also been exhaustively performed.[4,13] This has added greatly to the spectroscopic data base useful in refining force constants. High-resolution techniques have been used to measure the detailed rotational structure of some vibrational bands: IR absorption[14-16] and Raman[17-19] studies have given accurate values of moments of inertia and vibration-rotation interaction constants. Overlapping bands which have mutual perturbations (Fermi resonance) have also been probed.[20,21]

These spectroscopic experiments have been accompanied by harmonic force field parameterizations of successively increasing accuracy and sophistication. A prototypical, empirical fit by Whiffen[7] has been improved upon by Duinker and Mills,[8] Kydd,[9] and lately Ozkabak et al.[3] However, the ab initio calculation by Pulay, Fogarasi, and Boggs[1] does not predict the force constants which have been deduced from the empirical fits to experimental data.

Although the spectroscopic characterization of the fundamental vibrations of benzene in its ground ($\tilde{X}$) state is fairly complete experimentally, the same cannot be said of the first excited ($\tilde{A}$) state, since the frequencies of some modes are not yet known. Vibrational modes in the $\tilde{A}$ state have typically been studied by examining the vibrational structure associated with the $\tilde{A} \leftarrow \tilde{X}$ transition, which involves excitation of one of the delocalized π electrons into a π^* state. This transition is symmetry-forbidden in the electric-dipole approximation, but becomes slightly allowed with the aid of a vibrational excitation (of the correct symmetry); in other words it is "vibronically induced". The effect of the vibration is to mix the $\tilde{A}$ state slightly with a higher state to which transitions are allowed from the $\tilde{X}$ state.

Naturally, the first spectra were obtained with direct absorption techniques; features in these spectra were plentiful and difficult to assign conclusively. The use of the single vibronic level (SVL) fluorescence technique by Knight, Parmenter, and Schuyler[22] gave detailed information about dispersed fluorescence from selected vibrational levels in the $\tilde{A}$ state. With the $\tilde{X}$ state levels (final states) already largely understood, this made it possible to infer much more securely the vibrational characteristics of the emitting level in the $\tilde{A}$ state. A series of papers by Atkinson and Parmenter[23,24] is devoted to improving and summarizing the analyses of the $\tilde{A} \leftarrow \tilde{X}$ spectrum up to about 1978. At that time, direct absorption and related measurements had only provided $\tilde{A}$ state assignments of 11 of benzene's 20 vibrational modes. (There are 30 modes, but 10 are doubly degenerate.)

The application of lasers to the problem led to significant progress because multiphoton transitions, which require high light intensities, could now be investigated. This meant that the selection rules were different for different vibrational modes active in "inducing" a two-photon as opposed to a one-photon transition. Even a three-photon $\tilde{A} \leftarrow\leftarrow\leftarrow \tilde{X}$ spectrum has been reported,[25] and has been analyzed to give the assignment of an $\tilde{A}$ mode. The two-photon-excited fluorescence studies in benzene gas[26-34] permitted confirmation of the mechanism of the two-photon transition and an analysis of the strongpolarization dependence of its vibrational bandshapes on laser polarization. Two-photon-excited fluorescence with different polizations has also been studied on a benzene crystal at 4.2°K.[35] With these measurements, 4 more vibrational modes in the $\tilde{A}$ state were assigned and analyzed, with 4 left to be determined. Referring to Fig. 1, it is the frequencies of modes 3, 12, 13, and 20 in the $\tilde{A}$ state that have not yet been determined.

Just as in the studies of the $\tilde{X}$ state, additional useful information about the $\tilde{A}$ state is gained by studying isotopically substituted molecules. This work, undertaken largely by the Goodman group[36-39] is, however, not complete, and is perhaps not of obvious utility until more is known about C_6H_6 itself.

Naively, one would think that one- and two-photon spectroscopy should give access to all gerade and ungerade modes in the $\tilde{A}$ state. How do we account for the fact that 4 of 20 modes have not been detected? First, it is not enough to consider only the g/u aspect of the symmetry. The symmetry of benzene is so high that 3 of these unobserved modes are of symmetry classes not allowed in $\tilde{A} \leftarrow \tilde{X}$ transitions with one photon or 2 photons of the same frequency. The last unobserved mode, a C-H stretching mode, is symmetry-allowed in two-photon transitions but is simply too weak to be observed.

As part of an experiment to study overtones of C-H stretches in the cold benzene molecule,[40] we used infrared-ultraviolet double resonance to study several previously unobserved vibrational levels in the $\tilde{A}$ state of benzene. As a result we were able to determine frequencies of two hitherto unobserved modes (3 and 20) and confirm the assignment of a third (19), which has been a subject of controversy. Our assignments also support Pliva's analysis[41] of the fundamental C-H stretch associated with the $\tilde{X}$ state of benzene.

A schematic diagram depicting our IR + UV two-photon excitation of the C-H stretching vibrations in the $\tilde{A}$ state is shown in Fig. 2(a). In this paper we use the standard spectroscopic notations ν_i'', ν_i' to denote the frequency of the ith vibrational mode in the ground ($\tilde{X}$) and excited

($\tilde{A}$) states, respectively. The label $i_m j_n\ldots$ ($i^m j^n\ldots$) describes vibrational levels in the ground (excited) electronic state with m quanta of mode i, n quanta of mode j, etc. The transition frequency between the states $i_m j_n$ and $i^k j^\ell$ is compactly described as $i^k_m j^\ell_n$. Also, here we invent the notation CH_m (CH^m) to indicate a generic IR-active C-H stretching mode with m quanta in the $\tilde{X}$ ($\tilde{A}$) state. In Fig. 2, we assume (not true in the case of benzene) for simplicity that the zero-vibration UV transition 0^0_0 is allowed. The CH^1_0 transition is weak or forbidden. But there is nothing to prevent the CH^1_1 transition, which is actually just the 0^0_0 transition with the C-H stretching mode as a spectator. To excite the molecule to CH^1, we can first create the CH_1 population with IR excitation at $\nu_{IR} = \nu''_{CH}$ followed by UV excitation at $\nu_{UV} = CH^1_1$. The excited-state C-H stretching frequency is given by $\nu'_{CH} = \nu''_{CH} + CH^1_1 - 0^0_0$.

This is a logical extension of the procedure of analyzing "hot bands". Vibrational levels whose energies are below ~ 1000 cm^{-1} have significant thermal populations; their fractional Boltzmann populations at room temperature are at least e^{-5} ~ 1%, since kT ~ 200 cm^{-1}. It is not necessary to use a laser to pump populations into these levels. The thermal populations of C-H stretching states at ~ 3000 cm^{-1} are however extremely small at room temperature.

Let us now see how one goes about getting an IR-UV double resonance spectrum. We fix the IR frequency at ν''_{CH} and turn the IR light beam alternately on and off so that the CH_1 population is modulated. Then we expect to see an enhanced absorption at CH^1_1, and a diminished absorption at 0^0_0. The spectrum we expect in this simple example is shown in Fig. 2(b); the modulated UV absorption vs. ν_{UV} is sketched.

In this example $\nu'_{CH} > \nu''_{CH}$, so that $CH^1_1 > 0^0_0$. Also, the intensity ΔI_{CH} of the double-resonance signal is often less than ΔI_o, that of the ground-state depletion signal, for the following reasons. First, the Franck-Condon factor $|\langle CH^1|CH_1\rangle|^2$ is less than 1, since the mode ν'_{CH} is expected to be somewhat different from the mode ν''_{CH}. After all, the force constants are different in the two electronic states. Second, when pulsed lasers are used with a time delay between the IR and UV light pulses, there is a chance for the population in the CH_1 state to relax to other levels although the radiative lifetimes are often long compared to IR-UV pulse delays.

In our experiment we used a supersonic molecular beam as the sample. UV absorption measurements on such a "thin" sample are difficult. Our way around that difficulty was to use resonantly-enhanced two-photon ionization (R2PI). Molecules which have been resonantly excited to levels in the $\tilde{A}$ state are ionized by photons from the same beam. The ion signal is nearly proportional to the $\tilde{A}$ state population and is easy to detect and measure.

While an experiment such as this could be done with a static gas sample, the use of a supersonic molecular beam has an important advantage. With proper supersonic expansion, the molecules in the beam are "rotationally cold", with their rotational state distribution roughly described by a temperature $T_{rot} \sim 5$°K. The width of the "rotational envelope" associated with each vibrational band is greatly reduced, from ~ 30 cm^{-1} at T_{rot} ~300 °K to ~ 4 cm^{-1} at ~ 5°K. As a result, spectra which are horribly congested at room temperature take on a much more "sparse" appearance. This both increases the signal strength and makes both the IR and UV spectra easier to analyze. With given IR and UV laser bandwidths less than 1 cm^{-1}, only a small fraction of the ground state rotational distribution is excited to the CH_1 state and detected with the CH_1^1 transition. This fraction increases as the laser bandwidths overlap a larger portion of the rotational envelope.

II. EXPERIMENTAL

Figure 3 shows the salient components of our apparatus. Our sample was a supersonic beam formed by passing argon gas at 200 torr through a -30°C bubbler which contained frozen benzene. It proceeded into the 10^{-7} torr experimental chamber via a Lasertechnics[42] LPV pulsed valve equipped with a 0.5 mm diameter nozzle, a region of differential pumping, and a skimmer. Infrared and ultraviolet laser beams were loosely focused, and overlapped. They crossed the molecular beam inside a set of ion extraction plates. The ions generated by R2PI passed through a time-of-flight mass spectrometer and were detected with a Johnston electron multiplier.[43] We used a gated integrator to accumulate the ion signal for several laser shots.

Independently triggerable pulsed Nd:YAG laser systems[44] generated the tunable UV and IR frequencies required. Each laser could generate 700-mj, 9-nsec, 9394-cm^{-1} (1.06 μm) pulses at a rate of 10 Hz. The frequency-doubled output of one laser was used to pump a dye laser with LDS 698 or LD 700 dye,[45] to yield an output around 14000 cm^{-1}. This dye laser output was frequency-doubled in an automatically-tracked, angle-tuned KDP crystal and the resulting UV light was mixed with the fundamental Nd:YAG laser beam in yet another KDP crystal to give the ~ 38000 cm^{-1} UV frequency we actually used. The frequency-doubled output of the other Nd:YAG laser was used to pump another dye laser with LDS 821 dye[45] to yield an output around 12400 cm^{-1}. This dye laser output was mixed with the fundamental Nd:YAG laser beam in an automatically- angle-tuned $LiNbO_3$ crystal to generate an IR beam of ~1 mj/pulse at 3000-3100 cm^{-1}. This energy was sufficient to saturate the IR transitions, as expected on the basis of reported cross sections.[13] The resolution achieved with our lasers was 1 cm^{-1} in the IR and in the UV. The laser frequencies were calibrated to better than 1 cm^{-1} by measuring the accurately known spectral lines of neon with optogalvanic spectroscopy[46] and those of methane with photoacoustic spectroscopy.

A digital computer recorded ion signal levels, scanned laser wavelengths, and actuated a shutter which was used to turn the IR beam on and off every few sec. Our Nd:YAG pump lasers had a relative timing jitter of several nsec. In order to eliminate jitter-induced fluctuations in the R2PI signal, we made sure that the pump (IR) pulse always led the probe (UV) pulse. This guaranteed that the molecules received the complete dose of infrared light before being probed. A relative delay of ~15-20 nsec in triggering the UV laser with respect to the IR laser was sufficient. Repopulation of the vibrational ground state in ~ 20 nsec was insignificant, since the 3000-cm^{-1} states have radiative lifetimes of the order of msec.

A chopper operating at 0.3 Hz was used to turn the IR beam on and off. With the shutter in the IR beam closed, no molecules were pumped. With it open, the ground state population was depleted, and the CH_1 population was enhanced. Chopping the IR beam with the shutter thus imposed a modulation on the populations of the ground-state and the CH_1 state, and hence the ion (probe) signal. With the UV light fixed to ionize ground-state molecules, the amplitude of the probe signal modulation vs. IR frequency gave us the anticipated IR absorption spectra. On the other hand, fixing the IR excitation to create a population in a given mode and scanning the UV laser yielded the IR-UV double resonance spectra.

III. RESULTS

Our presentation of the results will be in three stages: first we will display R2PI spectra of portions of the $\tilde{A} \leftarrow \tilde{X}$ band as they appear without IR excitation. We will explain the characteristics of this electronic transition insofar as they pertain to this experiment. Second, we will show an IR spectrum of the fundamental C-H stretching vibrations, and describe a previous interpretation of its features. Finally, a series of spectra related to the IR-induced UV transitions will be presented.

A. R2PI Spectra

Our R2PI spectra, involving resonant transitions around 6^0_1 and 6^1_0 in the absence of infrared excitation, are shown in Figs. 4(a) and (b), respectively. It is seen that the 6^1_0 transition, saturated in our spectrum, is the dominating feature. It is at least 20 times more intense than the neighboring 16^2_0 band. The "rotational temperature" was determined to be ~ 5 °K and the "vibrational temperature" ~ 200 °K. Figure 4(c) is a corresponding energy level diagram illustrating these resonant transitions. It contains detail of hot bands and vibrational angular momentum splittings but does not include some weak transitions also observed in the R2PI spectra. The 0^0_0 transition around 38086 cm^{-1} is forbidden and hence was not observed. The spectral assignments are those derived from the recent molecular beam work of Stephenson et al.;[47] assignments not provided in that work are taken from the earlier study by Atkinson and Parmenter.[23]

There are many symmetry operations in the benzene molecule, and the notation used to describe the wavefunctions accordingly has several elements: a letter, a numerical subscript, and the usual g (gerade) or u (ungerade) subscript to indicate the parity. Figure 1 is a picture of the normal modes of benzene with their symmetry designations. We use capital letters to represent electronic wavefunctions and lower-case letters for vibrational wavefunctions. Letters A, B, and E describe wavefunctions of different symmetries with respect to rotation about the sixfold symmetry axis. Following the phase convention of Atkinson and Parmenter,[24] a $2\pi/6$ rotation about this axis is equivalent to multiplying the wavefunction by a phase factor $e^{-i\theta}$, with $\theta = 0$ for A, and π for B functions, as can be seen in Fig. 1. For the doubly degenerate modes E the $2\pi/6$ rotation causes a phase change of $2\pi/6$ in the wavefunction for the E_1 modes and $4\pi/6$ for the E_2 modes. When applied to the A and B states, the subscript 1 or 2 indicates even or odd behavior with respect to a rotation of π about an axis containing two carbon atoms.

The following multiplicative properties then apply:[10] $g \cdot g = u \cdot u = g$; $g \cdot u = u$. For A and B states, 1 and 2 behave analogously: $1 \cdot 1 = 2 \cdot 2 = 1$; $1 \cdot 2 = 2$. For the rotational symmetry, $A \cdot A = B \cdot B = A$; $A \cdot B = B$, $A \cdot E_1 = E_1$, $A \cdot E_2 = E_2$, $B \cdot E_1 = E_2$, and $B \cdot E_2 = E_1$. Also, $E_1 \cdot E_1 = E_2 \cdot E_2 = A_1 + A_2 + E_2$; $E_1 \cdot E_2 = B_1 + B_2 + E_1$.

Descriptive names have been applied to several of the modes. For example, ν_1 (a_{1g}), in which the molecule expands and contracts uniformly, is the "breathing" mode. ν_2 is the C-H stretching analog to ν_1, which is more a C-C stretching mode. The e_{2g} modes ν_6 - ν_9 tend to "squash" the molecule into a two-fold symmetric shape. Similarly, a threefold-symmetric "squashing" of the molecule occurs when b_{2u} modes are excited. e_{1u} vibrations cause the sets of carbon and hydrogen atoms to "slosh" with respect to each other, and produce a varying electric dipole moment which is the source of the infrared activity of these modes.

The selection rules for the electronic transition are found by evaluating the matrix element of the dipole moment operator $\langle\tilde{A}|\vec{\mu}|\tilde{X}\rangle$. The symmetry of $\langle\tilde{A}|\vec{\mu}|\tilde{X}\rangle$ must be A_{1g} in order for the matrix element to be nonzero. We already know that the symmetry species of $\tilde{A}$ and $\tilde{X}$ are B_{2u} and A_{1g}, respectively. Also, the in-plane dipole moment of $\vec{\mu}$ has E_{1u} symmetry. It is readily checked that $B_{2u} \cdot E_{1u} \cdot A_{1g} = E_{2g}$, not A_{1g}, so the $\tilde{A} \leftarrow \tilde{X}$ transition is formally forbidden. However, as the molecule vibrates, its electronic wavefunction is no longer purely B_{2u} in the $\tilde{A}$ state, or A_{1g} in the $\tilde{X}$ state. The electric dipole moment matrix element $\langle\mu\rangle = \langle\tilde{A}|\vec{\mu}|\tilde{X}\rangle$ can be expressed with the perturbation expansion

$$\langle\mu\rangle = \langle\mu\rangle\Big|_o + \sum_i \frac{\partial\langle\mu\rangle}{\partial Q_i}\Big|_o Q_i + \sum_{i,j} \frac{\partial^2\langle\mu\rangle}{\partial Q_i \partial Q_j}\Big|_o Q_i Q_j + \cdots$$

In this (Herzberg-Teller) expansion, the Q's represent normal coordinates and the constants are evaluated at the equilibrium geometry. The overall symmetry of each of the terms involving derivatives of $\langle\mu\rangle$ is the product of the symmetries of $\langle\mu\rangle|_o$ and the normal modes Q. We have just shown that $\langle\mu\rangle|_o$ has E_{2g} symmetry and that its magnitude is zero. In order to obtain A_{1g} symmetry for the derivative terms of $\langle\mu\rangle$, it is therefore necessary for Q_i (or Q_iQ_j) to have e_{2g} symmetry.

In this context, ν_6 is by far the most effective vibration that can induce the $\tilde{A} \leftarrow \tilde{X}$ transition because it squashes the ring the most. To zeroth order, the $\tilde{A} \leftarrow \tilde{X}$ spectrum is described by the selection rule $\Delta v_6 = \pm 1$. In the following, we will only be concerned with transitions involving $\Delta v_6 = \pm 1$.

Qualitatively, the $\tilde{A} \leftarrow \tilde{X}$ transition promotes a C-C π-bonding electron into an antibonding (π^*) state. The strength of the bonds holding the ring together is weakened, and the ring expands; this can be considered as setting the molecule into motion in the ν_1 mode. In fact, the strongest features in the $\tilde{A} \leftarrow \tilde{X}$ spectrum are the $6^1_0 1^n_0$ transitions, where n ranges from 0 to about 4. These transitions are spaced by ~ $\nu_1' = 923$ cm^{-1}. Interestingly, the states with 1 quantum of ν_1 in the $\tilde{X}$ and $\tilde{A}$ states are nearly orthogonal, and the intensity of a transition such as $6^1_0 1^1_1$ is at least 10 times smaller than 6^1_0 or $6^1_0 1^m_0$, where m = 0,2,3.[48] The forces which prevent out-of-plane motion are also much weaker in the $\tilde{A}$ state than in the $\tilde{X}$ state; frequencies of some out-of-plane modes are roughly half their $\tilde{X}$ state values. These out-of-plane normal modes (4, 5, 10, 11, 16, and 17) therefore have considerably different displacements in the two states. Within one or the other of the two electronic states, the vibrational modes have the usual orthonormal properties: $\langle i_m | i_k \rangle = \delta_{mk}$ and $\langle i_m j_n | i_k j_\ell \rangle = \delta_{mk}\delta_{n\ell}$, etc. Between the two states, the orthonormality is lost: $\langle i^m | i_k \rangle \neq \delta_{mk}$. Overlap integrals (Franck- Condon factors) such as $|\langle 16^1 17^1 | 0_0 \rangle|^2$ can then have appreciable values, and we have just mentioned that

$|\langle 1^1|1_1\rangle|^2 \ll 1$.

When we look at the spectrum of the 6^1_0 region we see that there are "hot bands" of the sort $6^1_0 16^1_1$ displaced to the red of the 6^1_0 band by $\nu''_{16} - \nu'_{16} \sim 161$ cm^{-1}. Here, the population in the 16_1 level is merely serving as another "ground state" for the 6^1_0 transition. If we did not know the value of ν'_{16} but knew ν''_{16}, we could find it from the relation $6^1_0 16^1_1 = 6^1_0 + \nu'_{16} - \nu''_{16}$.

A subtlety which pertains to our experiment is the shape of the rotational envelope of each band; it depends on the nature of the vibrational transition. When only one quantum of a degenerate vibration is involved, the band consists of a single peak, or a peak with a notch in the center if the resolution is sufficient to separate the P and R branches. Examples of this are the 6^0_1, $6^0_1 1^1_0$, and 6^1_0 bands, which have identical shapes. But when two or more quanta of degenerate vibrations are present, as in the 6^2_1 band at ~38520 cm^{-1} (Fig. 4b), the situation is more complex because the vibrations interact to produce a spectroscopically-observed splitting. (The weak $6^0_1 11^2_0$ band is masked by the 6^2_1 band.)

The presence of "vibrational angular momentum" can lift the degeneracy. The energy of a vibrational level is

$$E(v) = \sum_i \omega_i v_i + \sum_{i,j} x_{ij} v_i v_j + \sum_{i,j} g_{ij} \ell_i \ell_j . \tag{1}$$

ω_i is the harmonic frequency of mode i, x_{ij} is the anharmonicity between modes i and j, and g_{ij} is yet another anharmonic constant responsible for the energy dependence on the vibrational angular momentum quantum numbers ℓ_i, ℓ_j. When v_i quanta are present in a degenerate mode, ℓ_i can have the values v_i, $v_i - 2$, $v_i - 4$, ... $- v$. Figure 5(a) illustrates the effect of the vibrational angular momentum term $g_{ii}\ell_i^2$ on the energy levels. Other contributions to the energy are ignored because they don't depend on the vibrational angular momentum. Allowed ($\Delta\ell = \pm 1$) transitions are sketched. Only one final state energy is accessible from $\ell'' = 0$ (e.g. 6_0) states, but when $|\ell''| = 1$, two final state energies ($|\ell'| = 0,2$) are possible; their separation is $4g'_{ii}$. Figure 5(b) represents the 6^1_0 and 6^2_1 bands schematically, showing the $4g' \approx 7$ cm^{-1} splitting in the latter. Observed bandshapes are helpful in assigning transitions.

B. IR Spectra

The IR vibrational spectrum of benzene can be obtained by fixing the UV light at the 6^1_0 frequency and scanning the IR excitation. When the IR frequency is resonant with a transition to a vibrational state, population is removed from the 0_0 level and a dip in the R2PI ion signal results. Our spectrum in the region of the C-H stretching vibration obtained by this technique is shown in Fig. 6. There is only one infrared-active C-H stretching mode as predicted by the normal mode analysis, namely, ν_{20}. In the ground $\tilde{X}$ state, two combination modes have nearly the same frequency as the C-H stretch ν''_{20}, and are therefore in Fermi resonance with ν_{20}. They are anharmonically coupled with ν_{20} and each other, and have e_{1u} symmetry. Three transitions are then observed, corresponding to the absorption peaks at 3048, 3079, and 3101 cm^{-1}. These transitions originate from ν''_{20}, $\nu''_8 + \nu''_{19}$, and $\nu''_1 + \nu''_6 + \nu''_{19}$, respectively. The energy level diagram in Fig. 7 depicts how the levels shift due to anharmonic coupling, which also causes the new levels to have mixed character. To avoid confusion, we label them a", b", and c". Upon analysis of the double-resonance spectra, it will be possible to say what the dominant character of each level is. Each level can now serve as a ground state for UV transitions to levels in the $\tilde{A}$ state, so that more $\tilde{A}$-state vibrational levels can be examined. This and the chance to unravel the details of the C-H stretching Fermi resonance add a new dimension to the already interesting challenge of finding ν'_{20}.

C. IR-UV Double Resonance Spectra

We obtained double-resonance signals via each of the states a", b", and c", in both the 6^0_1 and 6^1_0 regions. This was done by fixing the IR excitation to pump the desired level and scanning the UV frequency. Opening and closing the shutter in the IR beam modulated the populations of molecules in the ground and excited vibrational states. The modulation was thus also imposed on the R2PI signals, and its UV frequency dependence was the information we desired. The spectra we present are actually the ion signals observed with the IR excitation on, minus the signals with it off. Thus all the features are due, in some way, to IR pumping.

Because the IR-excited levels a", b", and c" all have mixed character, it is expected that many transitions should exist in the UV spectra. The level $|a''\rangle$, for example, is actually $\alpha|20_1\rangle + \beta|8_1 19_1\rangle + \gamma|1_1 6_1 19_1\rangle$, with $\alpha^2 + \beta^2 + \gamma^2 = 1$, and $|\langle 20^1|a''\rangle|^2 \sim \alpha^2$, $|\langle 8^1 19^1|a''\rangle|^2 \sim \beta^2$, and $|\langle 1^1 6^1 19^1|a''\rangle|^2 \sim \gamma^2$. We assume that the Fermi resonance is quite different in the $\tilde{A}$ state with very different coefficients α, β, and γ. Then $|\langle b'|a''\rangle|^2 \neq 0$, etc. The picture in Fig. 2 (the double-resonance scheme) can be modified to reflect the state mixing: the CH_1 level then includes a", b", and c", and the CH^1 level splits into a',

b', and c'. Accordingly, each (a'', b'', or c'') in the $\tilde{X}$ state level could have transitions to three different $\tilde{A}$ state levels. A sketch of this situation is shown in Fig. 8(a). Note that since the doubly resonant transitions start from the common ground state level, $\nu_{IR} + \nu_{UV}$ for the transitions depends only on the energies of the final states. Thus, the UV transitions from the $\tilde{X}$ levels to a particular final state can be readily identified if the UV spectra are presented with the horizontal axes lined up to represent the sum of the IR and UV frequencies, as shown in Fig. 8(b). We have not included in Fig. 8(b) features due to depletion of the 0_0 level. Also, it is assumed that the strongest transitions come from $\langle a''| \rightarrow \langle a'|$, $\langle b''| \rightarrow \langle b'|$, and $\langle c''| \rightarrow \langle c'|$ because $|\langle a'|a''\rangle|^2 \gg |\langle a'|b''\rangle|^2$, etc. The top UV spectrum is expected when the IR excitation pumps the a'' transition, the middle spectrum is obtained with the b'' level populated, and the bottom spectrum shows transitions from the c'' state.

Our observed IR-UV double resonance spectra, arranged in the fashion of Fig. 8(b), are presented in Figs. 9 (for the 6^0_1 region) and 10 (for the 6^1_0 region). Because more transitions are actually present and depletion of the ground level population can give rise to additional features, the spectra appear more complicated, but can still be well understood after analysis following the approach outlined above, as we shall see.

In the R2PI spectra (Figs. 4ab) obtained with no IR excitation, each peak comes from a thermally populated $\tilde{X}$ vibrational level which can potentially be depleted by IR excitation. By looking at the dips in the double-resonance spectra (Figs. 9,10) one can see which of the thermal levels have their populations depleted by IR pumping at $\nu_{a''}$,

$\nu_{b''}$, and $\nu_{c''}$. The dips in the spectra of Figs. 9 and 10 are labelled according to their ground state vibrational levels. Peaks, on the other hand, are assigned and labeled according to their final state identities. It is seen that, in addition to depopulating 0_0, the IR excitations also depopulated the 11_1 and 16_1 levels. This is because the hot-band excitations of the a", b" and c" modes from 11_1 and 16_1 also occur at ν_a'', ν_b'', and ν_c'', respectively. The 6_1 level was depopulated by ν_a'' and ν_c'' excitations, but not by $\nu_{b''}$ excitation. The latter happens because the hot-band excitation $b''6_1 \leftarrow 6_1$ has a frequency red-shifted by ~ 3 cm^{-1} from the ground-state excitation $b'' \leftarrow 0_0$.[49] In Fig. 10, at the peak of the 6^1_0 transition, the detector was saturated by the huge ion signal whether the IR excitation was on or off, but at the wings of the peak, the detctor was able to record the IR-induced change in the 0_0 population, thus giving rise to a pair of dips.

We shall now try to account for all of the strong features, and a few of the weak ones, in the analysis.

IV. ANALYSIS

The presence of the C-H stretching Fermi triad is fortuitous and fascinating. Through it we have access, with double resonance, to a great many vibrational levels in the $\tilde{A}$ state. None of these levels has been previously detected, and we have a chance to determine the frequencies of the modes which make up the combination levels a', b', c'. Since we will be using the values of several vibrational frequencies in our transition assignments and calculations of newly-determined frequencies, we present in Table I an up-to-date list of the known frequencies in the $\tilde{X}$ and $\tilde{A}$ states. Some of these are known very accurately, having been determined with high-resolution laser spectroscopy. Others have been deduced in 1956 by Brodersen and Langseth[13] or estimated from observations of slightly-allowed transitions in benzene derivatives with lower symmetry. We have cited original sources of the vibrational frequency determinations and give the frequencies to the nearest 0.1 cm^{-1} if they are so reliably known. Suspicious or indirectly determined frequencies are enclosed in parentheses.

The first goal is to assign the UV transitions from the IR-excited levels a", b", and c". From earlier spectroscopic analysis,[13] it is known that a", b", and c" are mixtures of the 20_1, $8_1 19_1$, and $1_1 6_1 19_1$ states, as indicated in Fig. 7. For the benzene $\tilde{A} \leftarrow \tilde{X}$ UV transitions, the selection rules discussed in Sec. III.A. require $\Delta v_6 = \pm 1$ and Δv_1 = any integer, but $v_1' = v_1'' = 1$ would lead to a weak transition because of the small Franck-Condon factor. Thus, transitions from a", b", c" to a', b', c' (which are mixtures of 20^1, $8^1 19^1$, and $1^1 6^1 19^1$) shown in Fig. 8(a) are not allowed. We therefore consider only the ν_6-vibration-assisted transitions in the 6^1_0 and 6^0_1 regions. Figure 11 describes those upper states in $\tilde{A}$ that we believe we have observed in our spectra in Figs. 9 and 10. We assume in Fig. 11 that state mixing due to anharmonic vibrational coupling is not appreciable so that the states in $\tilde{A}$ retain more or less their pure mode character. This is largely vindicated by the analysis, as we shall see.

Figure 11(a) depicts the UV transitions in the 6^1_0 region with $\Delta v_6 = 1$ and $\Delta v_1 = 0$. Since the initial states involve 20_1, $8_1 19_1$, and $1_1 6_1 19_1$, the final states are thus $6^1 20^1$, $6^1 8^1 19^1$, and $1^1 6^2 19^1$. Figure

11(b) shows the transitions in the 6^0_1 region. The only final state that can be reached from a", b", and c" with $\Delta v_6 = -1$ and $\Delta v_1 = 0$ is $1^1 19^1$. Coincidentally, the $6^2 19^1$ state is near $1^1 19^1$, and is accessible via a $\Delta v_6 = +1$, $\Delta v_1 = -1$ transition.

The energy levels in Fig. 11 are plotted as a function of the total energy $\nu_{IR} + \nu_{UV}$, which can be identified with the frequency scale of Figs. 9 and 10, except for a 0^0 constant offset. Energies of these vibrational levels in the excited electronic state can now be expressed in terms of the vibrational frequencies of ν_1', ν_6', ν_9', ν_{19}', and ν_{20}'. The first three are known from previous spectroscopic work (see Table I), thus allowing ν_{19}' and ν_{20}' to be determined from our spectra.

Figure 11 also shows splittings of the levels associated with $v_6' = 2$ and $v_6' = v_8' = 1$, due to the presence of vibrational angular momentum (see Fig. 5 and accompanying discussion). Theoretically, splittings could also be induced by vibrational angular momenta associated with modes 19 and 20. However, since these modes mainly involve motion of the H atoms, they cause little distortion of the carbon ring and hence have small vibration-rotation interactions. We can therefore ignore the resulting small splittings.

The transitions which are predicted from the selection rules to be strongest are shown in Fig. 11 by heavy lines. In the manner of Fig. 8(b), each final level can be identified with a trio of vertically-aligned peaks in Fig. 9 or Fig. 10, corresponding to IR excitations of the three states a", b", and c". Beginning with the 6^0_1 region (Fig. 9), we can identify, from a frequency estimate, the intense peak at $E_{vib}' \approx 2445$ cm^{-1} as the $6^2 19^1$ level. It is a doublet, as predicted, and the splitting is ~ 9 cm^{-1}, roughly in agreement with the 7 cm^{-1}

splitting predicted in the model of Fig. 5. The $1^1 19^1$ level is expected to appear as a weak singlet at ~ 120 cm^{-1} to the red of the $6^2 19^1$ doublet. Indeed, it appears, at $E'_{vib} \approx 2330$ cm^{-1} in Fig. 9.

Continuing into the 6^1_0 region (Fig. 10), the peak at $E'_{vib} \approx 3430$ cm^{-1} should correspond to the $6^1 8^1 19^1$ final level. It should appear as a doublet, as most clearly discerned in the a" spectrum in Fig. 10. Since the value of the vibrational angular momentum coupling constant $g'_{6,8}$ in Eq. (1) is not known, the magnitude of the splitting is not predicted.

Thus the energies of $1^1 19^1$, $6^2 19^1$ and $6^1 8^1 19^1$ are found. Only that of $6^1 20^1$ is yet to be found. There are two relatively intense peaks at $E'_{vib} = 3580$ and 3618 cm^{-1} in each spectrum in Fig. 10. They have a nearly constant intensity ratio of ~ 2, and must correspond to two related final states. Since both appear in the neighborhood of $6^1 20^1$, and are optically accessible via $\Delta v_6 = +1$ transitions, we postulate that they arise from a Fermi resonance between $6^1 20^1$ with another level (either $6^1 13^1$ or $6^1 8^1 14^1$). These levels are not noticeably split by vibrational angular momentum interactions.

With the positions of the $1^1 19^1$ and $6^2 19^1$ combination levels secured, it is now possible to determine the frequency ν'_{19} by knowing ν'_1 and ν'_6. We consider two different approximations, both ignoring anharmonic shifts of levels involving v'_{19}: (a) $\nu'_{19} \approx 1^1 19^1 - 1^1 = (1^1 19^1 - 0^0) - \nu'_1 = 2330$ cm^{-1} $- 923$ cm^{-1} $= 1407$ cm^{-1} and (b) $\nu'_{19} \approx 6^2 19^1 - 6^2$. In the latter case, the 6^2 state has two vibrational angular momentum components, $\ell' = 0$ and $\ell' = 2$. From the relation $E(v) = \Sigma\, \omega_i v_i + \Sigma\, x_{ij} v_i v_j + \Sigma\, g_{ij} \ell_i \ell_j$, with $\omega'_6 = 519.0$ cm^{-1}, $x'_{6,6} = 0.7$ cm^{-1}, and $g'_{6,6} \approx 1.7$ cm^{-1},[24] we obtain 6^2 $(\ell' = 0) - 0^0 \cong 1041$ cm^{-1} and

6^2 ($\ell' = 2$) - $0^0 \cong 1048$ cm^{-1}. We then find $\nu'_{19} = 6^2 19^1 - 6^2 = 2443 - 1041$ cm^{-1} = 1402 cm^{-1} for $\ell' = 0$ and $\nu'_{19} = 2452 - 1048 = 1404$ cm^{-1} for $\ell' = 2$. The averaged value of ν'_{19} determined from all these estimates is 1405 cm^{-1}, in fair agreement with Hochstrasser's recent assignment[35] of $\nu'_{19} = 1400$ cm^{-1}, from a two-photon-induced fluorescence spectrum of a benzene crystal at 4.2°K, considering that the gas-to-crystal shift can easily exceed ~ 10 cm^{-1}.

The frequency of ν'_{19} can be used with the value of ν'_6 and ν'_8 to predict the position of the $6^1 8^1 19^1$ level: $E'_{vib} \approx \nu'_6 + \nu'_8 + \nu'_{19} = 3442$ cm^{-1}. This is ~ 12 cm^{-1} higher than the observed position at $E'_{vib} \approx 3430$ cm^{-1}; an anharmonic shift due to interactions between the three modes ν'_6, ν'_8 and ν'_{19} could easily account for the difference.

We now wish to deduce ν'_{20} from the doublet we have assigned to be associated with $6^1 20^1$. The final states of the doublet are believed to originate from $6^1 20^1$ and another state (either $6^1 13^1$ or $6^1 8^1 14^1$) to which the transitions from a", b", and c" have zero intensity. If W is the coupling matrix element between $6^1 20^1$ and the other state, ΔE_o and ΔE the energy separations between the two states before and after taking into account the coupling, respectively, and R is the intensity ratio of the two observed peaks, then Daunt and Shurvell[50] have shown that

$$\frac{W}{\Delta E} = \frac{\sqrt{R}}{R + 1} ,$$

$$\frac{\Delta E_o}{\Delta E} = \frac{R - 1}{R + 1} .$$

The more intense peak is associated with the perturbed $6^1 20^1$ state. Using these equations with the observed $\Delta E = 38$ cm^{-1} and $R = 2$, we find $\Delta E_o \approx 13$ cm^{-1} and $W \approx 18$ cm^{-1}. Therefore, the original decoupled states should have vibrational energies of $E'_{vib} = (1/2)[(3618 + 3580) \pm 13] = 3605$ and 3592 cm^{-1}. The former is the vibrational energy of the decoupled $6^1 20^1$ state, and we find $\nu'_{20} = 6^1 20^1 - 6^1 = (6^1 20^1 - 0^0) - \nu'_6 = 3605$ cm^{-1} $- 521$ cm^{-1} $= 3084$ cm^{-1}. A possibility for the perturbing state is $6^1 8^1 14^1$. A harmonic prediction of its position is $E'_{vib} = \nu'_6 + \nu'_{18} + \nu'_{14} = 3607$ cm^{-1}; anharmonicity would make the actual position lower, and closer to the $E'_{vib} = 3592$ cm^{-1} location of the decoupled perturber. The $6^1 20^1$ and $6^1 8^1 14^1$ levels have the same symmetry and can interact; note that 20^1 (e_{1u}) and $8^1 14^1$ ($e_{2g} \cdot b_{2u} = e_{1u}$) also can interact. Another possibility for the perturber is $6^1 13^1$ ($e_{2g} \cdot b_{1u} = e_{1u}$) which can interact with $6^1 20^1$ ($e_{2g} \cdot e_{1u} = b_{1u} + b_{2u} + e_{1u}$) by symmetry. The frequency ν'_{13} would be $3592 - 521 = 3071$ cm^{-1}. This is quite different from the value ~ 3160 cm^{-1} predicted by Robey[5] and Krogh-Jespersen.[6]

In Figs. 9 and 10, we notice that the c" spectra (Figs. 9, 10) have 3 extra peaks at $E'_{vib} = 2477$, 3402, and 3522 cm^{-1}. They must arise from UV transitions from the c" state, but we seem to have already exhausted all possibilities. Recently, however, Pliva[41] has shown, experimentally and theoretically, that the C-H stretching fundamental region actually contains a Fermi tetrad instead of the triad a", b", and c". It is believed that the original c" state is nearly degenerate with $3_1 6_1 15_1$ and hence the two states mix and create two new states c''_1 and c''_2 at ~ 3101 cm^{-1} with only 1 cm^{-1} separation between them [see Fig. (12)]. The a" and b" states are, however, sufficiently far away not to be affected by $3_1 6_1 15_1$. In our IR excitation, because of the limited laser resolution, c_1'' and c_2'' were always simultaneously excited.

If we accept this picture of Pliva, the assignment of the extra peaks in the c" spectra would be straightforward. They should be ν_6-assisted $\tilde{A} \leftarrow \tilde{X}$ transitions, and must therefore involve the following final states: $3^1 15^1$ for $\Delta v_6 = -1$, $3^1 6^2 15^1$ for $\Delta v_6 = +1$, and $1^1 3^1 15^1$ for $\Delta v_6 = -1$ and $\Delta v_1 = +1$. These transitions have similar Franck-Condon factors and hence nearly equal intensities. The transition to $3^1 6^2 15^1$ ought to display a doublet or complex bandshape due to the presence of more than one vibrational angular momentum (ℓ') level in the $3^1 6^2 15^1$ final state. These expectations are completely fulfilled. We can indeed assign peaks in the c" spectra of Figs. 9 and 10 as transitions from c" to $3^1 15^1$ at $E'_{vib} = 2477$ cm^{-1}, to $1^1 3^1 15^1$ at $E'_{vib} = 3402$ cm^{-1}, and to $3^1 6^2 15^1$ (which has a complex bandshape; its high-frequency "notch" is assumed to be the band center) at $E'_{vib} = 3522$ cm^{-1}.

The mode frequency ν'_3 can now be determined, knowing $\nu'_1 = 923$ cm^{-1}, $\nu'_{15} = 1150$ cm^{-1}, and $\nu'_6 = 521$ cm^{-1} from Table I. From $E'_{vib} = 2477$ cm^{-1} for $3^1 15^1$, we deduce $\nu'_3 = 1327$ cm^{-1}; from $E'_{vib} = 3402$ cm^{-1} for $1^1 3^1 15^1$, $\nu'_3 = 1328$ cm^{-1}; and from $E'_{vib} = 3522$ cm^{-1} for $3^1 6^2 15^1$, $\nu'_3 \sim 1330$ cm^{-1}. Since the first value should be least affected by the neglect of anharmonic corrections to the total vibrational energy, it is the preferred one. Thus we pick $\nu'_3 = 1327$ cm^{-1}.

All the peaks in the double resonance spectra of Figs. 9 and 10 whose IR transitions originated from 0_0 level, have now been assigned. The remaining peaks can be associated with double resonances originating from some IR hot bands. Recalling that the 11_1 and 16_1

levels are thermally populated (see Sec. III), we expect that the IR-UV double resonance transitions to $6^2 19^1 11^1$ and $6^2 19^1 16^1$ should also appear in the spectrum of Fig. 9. Their positions are predicted to have shifted by ~ -160 cm^{-1} from the transitions to $6^2 19^1$, as estimated from Table I or the separation between 6^1_0 and the $6^1_0 11^1_1$/ $6^1_0 16^1_1$ features in Fig. 4(b). Figure 9 shows that there is indeed a weak doublet in the b" spectrum at E'_{vib} = 2280,2288 cm^{-1}, which is 163 cm^{-1} lower than the intense $6^2 19^1$ doublet at E'_{vib} = 2243,2252 cm^{-1}.

Relative intensities of the different peaks in the double-resonance spectra give information about the state mixing in the C-H stretching Fermi tetrad. For example, the relative intensities of the transitions from a", b", and c" to $6^1 8^1 19^1$ are determined by the squared matrix elements $|\langle 6^1 8^1 19^1 | \mu | a'' \rangle|^2$, etc. These in turn are proportional to the Franck-Condon factors $|\langle 8^1 19^1 | a'' \rangle|^2$ etc., because ν_6 is responsible for inducing the transition but ν_8 and ν_{19} are not. Also, because ν'_8 and ν'_{19} differ only slightly from ν''_8 and ν''_{19}, respectively, their mode displacements must be similar in the two electronic states. The relation $|\langle 8^1 19^1 | 8_1 19_1 \rangle|^2 \sim 1$ then holds. This in turn implies that $|\langle 8^1 19^1 | a'' \rangle|^2 \sim |\langle 8_1 19_1 | a'' \rangle|^2$. Then, the fact that the $6^1 8^1 19^1$ signal is largest from the a" state indicates that a" has more of the character of $8_1 19_1$ than b" or c".

Similarly, a" is found to have more ν''_{20} character than b" or c" because the a" spectrum has the biggest $6^1 20^1$ peaks. Following the same line of argument, we find b" has the most $6_1 1_1 19_1$ character (contradicting the early assignment of b" in the literature[12]). $c''_{1,2}$ contains a substantial admixture of $\nu''_3 + \nu''_6 + \nu''_{15}$, but also has contributions to its makeup from 20_1, $8_1 19_1$, and $1_1 6_1 19_1$.

Knowledge of the $\nu_1'' + \nu_6'' = \nu_{19}''$ "parentage" of the b" state is also useful in explaining the observed 3 cm^{-1} shift between b"$6_1 \leftarrow 6_1$ and b" $\leftarrow 0_0$ as described at the end of Sec. III. This occurs because b" has most of the ν_6'' character in the Fermi tetrad, and hence its anharmonic frequency shift due to interaction with 6_1 is the largest. It is known that anharmonic interaction within a mode is usually larger than that between modes. None of the a", b", or c" levels contains ν_{11}'' or ν_{16}'', so no appreciable shift of a", b", or c" is expected to be induced by interaction with ν_{11}'' or ν_{16}''.

This completes the analysis of the spectra. Since it was a long process, replete with detail, we summarize now the main points.

1. With IR excitation around 3000 cm^{-1} we have selectively created populations in the a", b", and $c_{1,2}''$ states. These states, which are in Fermi resonance, are derived from the zeroth-order states ν_{20}'', $\nu_8'' + \nu_{19}''$, $\nu_1'' + \nu_6'' + \nu_{19}''$, and $\nu_3'' + \nu_6'' + \nu_{15}''$.

2. We have observed UV transitions from each of these levels, and thereby managed to get a rough estimate of the makeup of each. Pliva's[41] analysis, which asserts that the b" state most nearly resembles $\nu_1'' + \nu_6'' + \nu_{19}''$, is confirmed. Also, the presence of $\nu_3'' + \nu_6'' + \nu_{15}''$ in the c" level, but not in the other levels, is proven.

3. We have evaluated the mode frequencies of ν_3', ν_{19}', and ν_{20}' in the excited electronic $\tilde{A}$ state, heretofore undetermined in gas-phase studies. They are $\nu_{19}' = 1405$ cm^{-1}, $\nu_3' = 1327$ cm^{-1}, and $\nu_{20}' = 3084$ cm^{-1}.

4. We have detected the existence of an $\tilde{A}$ state Fermi resonance which splits the $6^1 20^1$ level. The interfering state could be $6^1 8^1 14^1$ or $6^1 13^1$. If the latter is the case, it would give ν_{13}' a frequency of ~ 3071 cm^{-1}.

V. DISCUSSION

A. Review of in-plane force field problem

The new frequency assignments provide new insight into the chemical bonding and vibrational behavior of benzene in its $\tilde{A}$ ($^1B_{2u}$) state, and serve as a test of recently calculated force fields. We shall show that current $\tilde{A}$ state force fields may have been calculated with incorrect vibrational frequencies as input data.

It is hoped that through force constant fitting, and ab initio calculation, one could obtain the valence force constants that would describe the chemical bonds. Naively, finding the valence force constants proceeds in the following manner: the normal mode frequencies are used with the secular equation(s) to find the normal coordinates and symmetry force constants. A linear transformation is then used to find the valence constants. There are several reasons why this is a difficult task. Qualitatively, there are very few vibrational modes whose frequencies depend on only a small number of valence force constants. For example, the C-C stretching and C-H bending frequencies are similar, so the two types of modes tend to be mixed. Similarly, C-C-C angle bending modes are not too different in frequency from the C-C stretching modes, so they too are mixed. A great deal of data is necessary to be sure that a derived force field actually can reproduce observed frequencies and predict unobserved ones. The problem of providing enough data to determine a force field can in principle be solved by spectroscopic measurements on isotopically-substituted benzenes, which have the same chemical bonds and valence forces, but different normal modes and vibrational frequencies. Such a fully determined force field has recently been published[3] for the ground ($\tilde{X}$;

$^1A_{1g}$) state of benzene, resulting from a fit to 244 experimental data on various substituted benzenes. It is not in agreement with predictions[2] from ab initio calculations.

For future reference, Table II is a list of the in-plane modes, their experimental $\tilde{X}$ and $\tilde{A}$ state frequencies, and their $\tilde{A}$ state values calculated in 1977 by Robey and Schlag[5] and in 1984 by Krogh-Jespersen et al.[6] Both of the calculations are fits to experimental data. The Robey-Schlag field has salient errors in its prediction of ν_3' and ν_8', neither of which was known at the time. (Nor was ν_{12}', ν_{13}', or ν_{20}'!) With 17 valence force parameters, their force field reproduced the 8 known vibrational frequencies. The average error was only ~ 0.33%. Important spectroscopic developments occurred around and after the time of their work, causing the force field to be re-examined by Krogh-Jespersen et al. Especially relevant were the determinations of ν_{19}' and ν_8'. A description of these experiments follows.

B. Review of recent experiments and derivation of force field

Several experiments with two-photon excitation have been done, resulting in many reports of ν_{19}', predicted to be a mode that can induce the $\tilde{A} \leftrightarrow \tilde{X}$ transition. The first value, 1560 cm^{-1}, was found by Hochstrasser et al.,[26] who were actually observing the 14_0^1 band. Bray et al.[27] later found a distinct, weak peak near this 14_0^1 band and called it 19_0^1 with $\nu_{19}' = 1586$ cm^{-1}. Friedrich and McClain[28] revised this to $\nu_{19}' = 1579$ cm^{-1}. Wunsch et al.[29,30] pointed out that this extra peak was actually a rotational branch of the 14_0^1 band and managed to find $\nu_{19}' = 1213$ cm^{-1} in C_6D_6. Lombardi et al.[34] also found $\nu_{19}' = 1209$ cm^{-1} in C_6D_6; they estimated that $\nu_{19}' = 1330$ cm^{-1} in C_6H_6. However, it seems to us that the isotopic product rule[10]

$\nu_{18D}\nu_{19D}\nu_{20D}/\nu_{18H}\nu_{19H}\nu_{20H} = (m_H/m_D)\sqrt{(M_D/M_H)}$ could have been used to estimate this frequency more accurately. (The capital M's represent the total masses of the isotopic molecules.) $\nu'_{20H,D}$ was not known, but with the reasonable assumption that $\nu'_{20} = \nu''_{20}$ and knowing $\nu'_{18D} = 758$ cm^{-1}, $\nu'_{19D} = 1209$ cm^{-1}, and $\nu'_{18H} = 922$ cm^{-1}, one gets $\nu'_{19H} = 1430$ cm^{-1}, an answer nearly in agreement with the 1405 cm^{-1} value we have obtained. Wunsch et al.[32] correctly surmised that $\nu'_{19} \sim 1410$ cm^{-1}, and that the 19^1_0 band was buried under the intense $14^1_0 16^1_1$ band at 1408.0 cm^{-1}.[33] In spite of the fact that this latter band appears to be very sharp and narrow in the molecular beam spectrum of Sur et al.,[33] its width at the 10% height is ~ 6-7 cm^{-1}. It is therefore conceivable that the $14^1_0 16^1_1$ and 19^1_0 bands coincide. Hochstrasser et al.[35] also found $\nu'_{19} = 1400$ cm^{-1} in a 4.2°K benzene crystal. But since this last work, Aron *et al.*[51] and Sur *et al.*[33] have found reason to support the 1330 cm^{-1} value of Lombardi *et al*.[34] To resolve the controversy, a high-resolution two-photon $\tilde{X} \leftarrow \tilde{A}$ absorption spectrum around $E'_{vib} = 1410$ cm^{-1} should be obtained in a very cold molecular beam. By suppressing th $14^1_0 16^1_1$ peak via cooling, the 19^1_0 transition may become more distinct.

The ν'_8 frequency had long been sought, since as an e_{2g} mode ν_8 can induce the one-photon $\tilde{A} \leftarrow \tilde{X}$ transition. The 8^1_0 transition was discovered in 1983 by Otis et al.[25] by using three-photon fluorescence excitation spectroscopy. The assignment was confirmed by the one-photon absorption spectroscopy measurement of Muller and Knight,[52] and the final value $\nu'_8 = 1516$ cm^{-1} was obtained from the molecular beam spectrum of Stephenson et al.[47] This accurately determined value of ν'_8 made it worthwhile to revise the earlier force field calculations.

Still using 17 valence force constants, Krogh-Jespersen et al.[6]

recently were able to improve on the Robey-Schlag force field. Whereas Robey and Schlag had used input data from two isotopic benzenes C_6H_6 and C_6D_6, Krogh-Jespersen et al. used frequencies from six molecules C_6H_6, s-$C_6H_3D_3$, p-$C_6H_4D_2$, p-$C_6H_2D_4$, m-$C_6H_4D_2$, and C_6H_5D.

The value ν'_{19} = 1347 cm^{-1}, obtained by them from analyzing the work of Aron et al.[51] is unfortunately incorrect (our new value is 1405 cm^{-1}). It is not stated whether ν'_{19} was observed in the other five benzenes they studied. Their calculated ν'_{19} value of 1359 cm^{-1} is the only salient disagreement with current data on C_6H_6. The errors in ν'_3 and ν'_8 as determined by the Robey-Schlag field have been removed.

C. New perspective on $\tilde{A}$ state vibrations

In the molecular orbital description of the $\tilde{A} \leftarrow \tilde{X}$ transition, a π electron in the carbon ring makes a $\pi^* \leftarrow \pi$ bonding-to-antibonding transition. The carbon ring weakens, and the C-C bond length increases from 1.3974(10) Å to 1.4319(9) Å, a lengthening of .0345(15) Å.[31] Therefore, the carbon ring is easier to squash, twist, and stretch, as evidenced by the reductions in normal mode frequencies upon going from $\tilde{X}$ to $\tilde{A}$. This happens for all the out-of-plane modes, the "C-C-C angle-bending" (squashing) vibrations ν_6 and ν_{12}, and the "C-C stretches" ν_1, ν_8, and ν_{18}.

The nominally C-C stretching mode, ν_{14}, shows on the other hand a frequency <u>increase</u> of 260 cm^{-1}! Calculation of the frequency of this mode has always been problematic. Mikami and Ito[53] explain the observation by the argument that in the ground ($\tilde{X}$) state, its symmetry force constant and frequency are lower than those predicted by simple estimates.

The C-H σ bonds should not be strongly affected by the $\tilde{A} \leftarrow \tilde{X}$, $\pi^* \leftarrow$

π transition because their σ electrons are not part of the π cloud.[53] We expect that the C-H bending force constant could appear to be slightly less in the $\tilde{A}$ state than in the $\tilde{X}$ state, because bending a C-H bond also tends to cause some C-C stretching motion in the weakened carbon ring. This effect can be important in the normal mode analysis because the C-C stretching and C-H bending frequencies at 1000-1500 cm^{-1} are not widely separated: Many modes in that region have mixed C-C stretch/C-H bend characteristics. The C-H stretches, at ~ 3000 cm^{-1}, are however much more decoupled, and their force constants should be largely unaffected.

In addition to determining the 0.035 A increase in the C-C bond length caused by the $\tilde{A} \leftarrow \tilde{X}$ transition, Lombardi et al.[31] found that the C-H bond length change was zero, with an uncertainty of 0.005 A. Thus the C-H bond strength is expected to be about the same in the $\tilde{X}$ and $\tilde{A}$ states. Compared to the changes in the frequencies of the C-C stretching modes in going from $\tilde{X}$ to $\tilde{A}$ we have already mentioned, reductions in the "C-H bending" frequencies of ν_3, ν_9, ν_{15}, and ν_{19} should be rather small. Indeed, Table I shows that the "pure" bending mode ν_3 decreases by ~ 20 cm^{-1}; ν_9 goes down ~ 30 cm^{-1}, ν_{15} does not change, and ν_{19} loses ~ 80 cm^{-1}. The average reduction of these mode frequencies only amounts to ~ 2.5%.

Now we look at the C-H stretches ν_2, ν_7, ν_{13}, and ν_{20}. In the $\tilde{X}$ state their frequencies all fall within a 20 cm^{-1} range. Table I shows that ν_7 increases by only 20 cm^{-1} in the $\tilde{A}$ state. The 3077 cm^{-1} assignment of ν_7' is unambiguous because, as an e_{2g} mode, the ν_7-assisted $\tilde{A} \leftarrow \tilde{X}$ transition is easily detectable. Also, there are no other strong transitions near the 7_0^1 band. The values of ν_{20}'' (3065

cm^{-1}) and ν'_{20} (3084 cm^{-1}) also show a ~ 20 cm^{-1} difference. The small increase in the C-H stretching frequencies caused by the $\tilde{A} \leftarrow \tilde{X}$ transition is explained as follows: The $\pi^* \leftarrow \pi$ transition makes the π electrons in the C-C bonds repel each other slightly and shift into the C-H bonds, thereby strengthening them and increasing the C-H stretching frequency.

The 3130 cm^{-1} value of ν'_2 assigned by Atkinson and Parmenter[23] appears to be 56 cm^{-1}, instead of ~ 20 cm^{-1}, higher than ν''_2. This makes the assignment questionable. Mikami[53] has suggested that the 3130 cm^{-1} vibration in the $\tilde{A}$ state may actually correspond to the $2\nu_{14}$ mode: $2\nu_{14}$ has a_{1g} symmetry, the energy is almost exactly correct, and the Franck-Condon factor $|\langle 14^2 | 0_0 \rangle|^2$ is nonzero because mode 14 has different frequencies and spatial wave functions in the $\tilde{X}$ and $\tilde{A}$ states. In their extensive analysis of the $\tilde{A} \leftarrow \tilde{X}$ absorption spectrum, Atkinson and Parmenter[24] had found ν'_2 through identification of a progression which they assigned as $6^1_0 2^1_0 1^n_0$, where n ranges from 0 to 4. However, there is a slightly weaker progression 41 cm^{-1} lower. The lowest-frequency member occurs at 41700 cm^{-1}. If <u>this</u> were called $6^1_0 2^1_0$, we would have $\nu'_2 = 6^1 2^1 - 0^0 - \nu'_6 = 3093$ cm^{-1}. Since no assignment was proposed for these transitions, we suggest that <u>they</u> could be the $6^1_0 2^1_0 1^n_0$ bands, and claim that $\nu'_2 \approx 3093$ cm^{-1}. This value fits into the new picture and is ~ 20 cm^{-1} higher than ν''_2 at 3074 cm^{-1}.

Finally we consider ν'_{13}, unobserved to date because of its b_{1u} symmetry. Force field calculatins by Robey and Schlag, and by Krogh-Jespersen et al., put ν'_{13} at ~ 3160 cm^{-1}. However, this may not be reliable as the force field which yields this number has been constrained to reproduce what we believe to be an incorrect value of

ν_2'. Being a C-H stretching mode, it seems likely that ν_{13}' is also ~ 20 cm^{-1} higher than ν_{13}'', or $\nu_{13}' \cong 3077\ cm^{-1}$. This is about the value it would need to have to cause a Fermi resonance between the $6^1 20^1$ and $6^1 13^1$ levels, as we speculated in the Analysis section.

Here, we have determined the frequency (ν_{20}') of one of the four $\tilde{A}$ state C-H stretches. It and the other reliably-assigned mode frequency (ν_7') are both ~ 20 cm^{-1} higher than their $\tilde{X}$ state values. This fact has led us to scrutinize previous spectroscopic work and propose a reassignment of the frequency of a third C-H stretch (ν_2'), so that its behavior also follows the same pattern. It also allows us to predict the frequency of the fourth C-H stretch (ν_{13}') to be ~ 80 cm^{-1} lower than the force field calculations suggest. It would now be worthwhile to repeat the force field fitting with these augmented data and altered frequency assignments.

VI. CONCLUSION

We have used the powerful, elegant double-resonance technique to study a prototype intermediate size molecule (benzene) cooled in a supersonic expansion. The thorough work which has already been done on the $\tilde{X}$ vibrations and the $\tilde{A} \leftarrow \tilde{X}$ transition of benzene allowed us to make decisive assignments of several IR-pumping-induced UV transitions. With these assignments we were able to confirm, in a qualitative way, Pliva's analysis of the C-H stretching Fermi tetrad in the $\tilde{X}$ state. Also, we provided a determination of the gas-phase value of ν_{19}', the IR-active C-H bend, and the first observation in the $\tilde{A}$ state of ν_3, the "C-H libration", and of ν_{20}, the IR-active C-H stretch. The values of these frequencies are found to be $\nu_{19}' \cong 1405\ cm^{-1}$, $\nu_3' \approx 1327\ cm^{-1}$, and

$\nu_{20}' \approx 3084\ \text{cm}^{-1}$.

Observation of a Fermi resonance with the $6^1 20^1$ level led us to speculate that $\nu_6' + \nu_{20}'$ could be perturbed by $\nu_6' + \nu_8' + \nu_{14}'$, or $\nu_6' + \nu_{13}'$. If the latter were the case, it would determine the unobserved ν_{13}' frequency as ~ 3071 cm^{-1}.

A qualitative consideration of the valence forces at work in $\tilde{A}$-state benzene impelled us to assert that the C-H bonds are largely unaffected by the $\tilde{A} \leftarrow \tilde{X}$ transition. C-H stretching frequencies ν_2, ν_7, ν_{13}, and ν_{20} should increase uniformly by ~ 20 cm^{-1} in the $\tilde{A}$ state. ν_7 and ν_{20} fit this pattern. The longstanding assignment of ν_2', the totally symmetric C-H stretch, does not. A review of the data of Atkinson and Parmenter[24] supports our suspicion that ν_2' is really ~ 3093 cm^{-1}, 20 cm^{-1} above the $\tilde{X}$-state value. In this context, ν_{13}, the unobserved IR- and Raman-inactive b_{1u} C-H stretch could very well have a value of ~ 3070-3080 cm^{-1}.

The $\tilde{A}$ state force fields of Robey and Schlag[5] and Krogh-Jespersen et al.[6] do not reproduce our experimental results and disagree with our qualitative analysis of the benzene molecule in its first excited state. Our analysis shows that the $\tilde{A}$ state resembles the $\tilde{X}$ state to a higher degree than was thought. Fitting of force fields should be easier when the more realistic vibrational frequencies we now have are used as input data.

Even with new vibrational frequencies, the data are insufficient to completely determine a force field. Now that it is widely recognized[3] that a large spectroscopic data base is required for the attainment of a plausible fit, we hope that our technique, and variants of it, will be espoused in the quest for accurate data on hard-to-observe modes.

There are several ways in which this could proceed: (1) Study of the selectively deuterated benzenes, as has been done in the $\tilde{X}$ state, would provide extremely useful data on normal modes, frequencies, and assignments. (2) Higher resolution (~ .001 cm^{-1}) lasers could give well-resolved rotational structure, leading to the determination of vibration-rotation interaction (Coriolis) constants. These constants can be used as input data for force-field refinement calculations. (3) Different optical transitions could be employed: namely, (a) many IR-active modes in the ~ 1000 cm^{-1} region could be pumped with a CO_2 laser. (b) Raman pumping instead of IR pumping could be used to populate different $\tilde{X}$ state modes, as demonstrated by Esherick and Owyoung.[21] (c) The second step of the double-resonance excitation could be done with multiphoton transitions instead of single photon transitions. This would allow different $\tilde{A}$ levels to be studied, and would present the opportunity for polarization-dependence studies of transitions in the new modes. Clearly, there are many possibilities, each of which can lead to interesting information about the excited states of aromatic molecules.

A thorough understanding of the first excited state of a simple phenyl system could prove useful in several situations. Vibrations and their anharmonicity are thought to be important in mediating radiationless transitions. Radiationless decay is not thoroughly characterized in either the $\tilde{X}$ or $\tilde{A}$ states of benzene. Also, the electronic properties of phenyls help to determine the qualities of many molecules of photophysical and photochemical interest. For example, phenyl rings form the basis of many (e.g. laser) dyes. Enhancements in lasing efficiency and photochemical stability could perhaps be engineered with better knowledge of excited-state geometries and forces.[54-56]

We hope that the step we have taken toward understanding $\tilde{A}$ ($^1B_{2u}$)-state benzene better will encourage further calculations and spectroscopic inquiries.

VII. Acknowledgements

Thanks are due Prof. Josef Pliva and Prof. Lionel Goodman for helpful discussions and for communicating results prior to publication. This work was supported by the Director, Office of Energy Research, Office of Basic Energy Sciences, Materials Sciences Division of the U.S. Department of Energy under Contract No. DE-AC03-76SF00098.

References

[*] Also associated with Department of Physics, University of California, Berkeley, California 94720.

[†] Also associated with Department of Chemistry, University of California, Berkeley, California 94720.

(a) Permanent address: IBM Almaden Research Center, 650 Harry Rd., San Jose, California 95120-6099.

1. P. Pulay, G. Fogarasi, and J. E. Boggs, J. Chem. Phys. 74, 3999 (1981).
2. P. Pulay, J. Chem. Phys. 85, 1703 (1986).
3. A. G. Ozkabak, L. Goodman, S. N. Thakur, and K. Krogh-Jespersen, J. Chem. Phys. 83, 6047 (1985).
4. S. N. Thakur, L. Goodman, and A. G. Ozkabak, J. Chem. Phys. 84, 6642 (1986).
5. M. J. Robey and E. W. Schlag, J. Chem. Phys. 67, 2775 (1977).
6. K. Krogh-Jespersen, R. P. Rava, and L. Goodman, J. Phys. Chem. 88, 5503 (1984).
7. D. H. Whiffen, Phil. Trans. Roy. Soc. London, Ser. A 248, 131 (1955).
8. J. C. Duinker and I. M. Mills, Spectrochim. Acta 24A, 417 (1968).
9. R. A. Kydd, Spectrochim. Acta 27A, 2067 (1971).
10. E. B. Wilson, J. C. Decius, and P. C. Cross, Molecular Vibrations, (McGraw-Hill, New York, 1955).
11. E. B. Wilson, Phys. Rev. 45, 706 (1934); 46, 146 (1934).
12. G. Herzberg, Molecular Spectra and Molecular Structure. II. Infrared and Raman Spectra of Polyatomic Molecules (Van Nostrand, Princeton, NJ, 1945).

13. S. Brodersen and A. Langseth, Mat. Fys. Skr. Dan. Vid. Selsk. 1, (1) 1 (1956); 1, (7) 1 (1959).

14. J. Pliva and A. S. Pine, J. Mol. Spectrosc. 93, 209 (1982).

15. J. Pliva and J. W. C. Johns, Can. J. Phys. 61, 269 (1983).

16. J. Pliva and J. W. C. Johns, J. Mol. Spectrosc. 107, 318 (1984).

17. B. P. Stoicheff, Can. J. Phys. 32, 339 (1954).

18. A. B. Hollinger and H. L. Welsh, Can. J. Phys. 56, 974; 1513 (1978).

19. H. B. Jensen and S. Brodersen, J. Raman Spectrosc. 8, 103 (1979).

20. D. L. Snavely, V. A. Walters, S. D. Colson, and K. B. Wiberg, Chem. Phys. Lett. 103, 423 (1984).

21. P. Esherick, A. Owyoung, and J. Pliva, J. Chem. Phys. 83, 3311 (1985).

22. A. E. W. Knight, C. S. Parmenter, and M. W. Schuyler, J. Am. Chem. Soc. 97, 1993; 2005 (1975).

23. G. H. Atkinson and C. S. Parmenter, J. Mol. Spectrosc. 73, 20 (1978).

24. G. H. Atkinson and C. S. Parmenter, J. Mol. Spectrosc. 73, 31; 52 (1978).

25. C. E. Otis, S. G. Grubb, K. S. Haber, and A. C. Albrecht, Chem. Phys. Lett. 102, 145 (1983).

26. R. M. Hochstrasser, J. E. Wessel, and H. N. Sung, J. Chem. Phys. 60, 317 (1974).

27. R. G. Bray, R. M. Hochstrasser, and H. N. Sung, Chem. Phys. Lett. 33, 1 (1975).

28. D. M. Friedrich and W. M. McClain, Chem. Phys. Lett. 32, 541 (1975).

29. L. Wunsch, H. J. Neusser, and E. W. Schlag, Chem. Phys. Lett. 31, 433 (1975).

30. L. Wunsch, H. J. Neusser, and E. W. Schlag, Chem. Phys. Lett. 38, 216 (1976).

31. J. R. Lombardi, R. Wallenstein, T. W. Hänsch, and D. M. Friedrich, J. Chem. Phys. 65, 2357 (1976).

32. L. Wunsch, F. Metz, H. J. Neusser, and E. W. Schlag, J. Chem. Phys. 66, 386 (1977).

33. A. Sur, J. Knee, and P. Johnson, J. Chem. Phys. 77, 654 (1982).

34. J. R. Lombardi, D. M. Friedrich, and W. M. McClain, Chem. Phys. Lett. 38, 213 (1976).

35. R. M. Hochstrasser, C. M. Klimcak, and G. R. Meredith, J. Chem. Phys. 70, 870 (1979).

36. S. N. Thakur and L. Goodman, J. Chem. Phys. 78, 4356 (1983).

37. R. P. Rava, J. G. Philis, K. Krogh-Jespersen, and L. Goodman, J. Chem. Phys. 79, 4664 (1983).

38. L. Goodman and R. P. Rava, Advances in Laser Spectroscopy, Vol. 1, 21 (Heyden and Son, Philadelphia, 1982).

39. L. Goodman and R. P. Rava, Advances in Chemical Physics, I. Prigogine and S. A. Rice, eds.,Vol. 54, 177 (Wiley & Sons, New York, 1983).

40. R. H. Page, Y. R. Shen, and Y. T. Lee, to be published.

41. J. Pliva, private communication.

42. Lasertechnics, Inc., Albuquerque, New Mexico.

43. Johnston Laboratories, Towson, Maryland.

44. Quanta-Ray (Spectra-Physics, Inc.), Mountain View, California.

45. Exciton Chemical Co., Inc., Dayton, Ohio.

46. J. R. Nestor, Appl. Opt. 21, 4154 (1982).

47. T. A. Stephenson, P. L. Radloff, and S. A. Rice, J. Chem. Phys. 81, 1060 (1984).

48. C. S. Parmenter, K. Y. Tang, and W. R. Ware, Chem. Phys. 17, 359 (1976).

49. R. H. Page, unpublished results.

50. S. J. Daunt and H. F. Shurvell, J. Mol. Spectrosc. 62, 373 (1976).

51. K. Aron, C. Otis, R. E. Demaray, and P. Johnson, J. Chem. Phys. 73, 4167 (1980).

52. D. J. Muller and A. E. W. Knight, J. Phys. Chem. 88, 3392 (1984).

53. N. Mikami and M. Ito, J. Chem. Phys. 64, 3077 (1976).

54. M. Rinke, H. Güsten, and H. J. Ache, J. Phys. Chem. 90, 2661; 2666 (1986).

55. G. A. Reynolds and K. H. Drexhage, J. Org. Chem. 42, 885 (1977).

56. B. Kopainsky, P. Qiu, W. Kaiser, B. Sens, and K. Drexhage, Appl. Phys. B 29, 15 (1982).

Table I. Compilation of benzene $\tilde{X}$ ($^1A_{1g}$) and $\tilde{A}$ ($^1B_{2u}$) frequency assignments.

Mode[b]	$\tilde{X}$ (cm^{-1})[c]	Ref.[a]	$\tilde{A}$ (cm^{-1})[c]	Ref.[a]
1 (2)	993.1	HW	923.0	AP
2 (1)	3073.9	HW	(3130.1)[g]	AP
3 (3)	(1350)[d]	BL	1327 ± 3[hd]	
4 (8)	(707)[d]	BL	365	KPS
5 (7)	(990)[d]	BL	744.6	AP
6 (18)	608.1	HW	521.4	AP
7 (15)	(3056.6)[e]	HW	3077.2	KPS
8 (16)	1600[f]	EOP	1516	SRR
9 (17)	1177.8	HW	1147.7	AP
10 (11)	(847.1)[e]	HW	580.7	AP
11 (4)	674.0	SWCW	515-518[d]	AP
12 (6)	(1010)[d]	BL		
13 (5)	(3057)[i]	BL		
14 (9)	1309.8	TGO	1570.0	SKJ
15 (10)	1148.5	TGO	1149.9	SKJ
16 (20)	398.8	AP	237.5	AP
17 (19)	(967)[d]	BL	717.4	SKJ
18 (14)	1038.3	PJ	919.7	SKJ
19 (13)	1484.0	PJ	1405 ± 3[hd]	
20 (12)	3065[f]	PP; SWCW; BL	3084 ± 5[hfd]	

[a] AP means Atkinson and Parmenter[23]
BL means Brodersen and Langseth[13]
HW means Hollinger and Welsh[18]
EOP means Esherick, Owyoung, and Pliva[21]
SWCW means Snavely et al.[20]
TGO means Thakur, Goodman, and Ozkabak[4]
PJ means Pliva and Johns[15,16]
PP means Pliva and Pine[14]
SRR means Stephenson, Radloff, and Rice[47]
SKJ means Sur, Knee, and Johnson[33]
KPS means Knight, Parmenter, and Schuyler[22]

[b] Wilson numbering; Herzberg numbering in parentheses

[c] Quoted to the nearest 0.1 cm^{-1}; uncertain values in parentheses

[d] Derived from combination band analysis

[e] Uncertainty is > 0.1 cm^{-1}

[f] Deperturbed value; mode is in Fermi resonance

[g] Reassigned in this work to ~ 3093 cm^{-1}

[h] This work

[i] Estimate from isotopic product and sum rules

Table IIa. $\tilde{X}$ and $\tilde{A}$ state frequencies of in-plane modes.

Mode	Symmetry	Observed (cm^{-1})		Robey-Schlag[5]	Krogh-Jespersen et al.[6]
		$\tilde{X}$	$\tilde{A}$		
1	a_{1g}	993	923	923	921
2	a_{1g}	3074	~3093[a]	3129	3111
3	a_{2g}	1350[b]	1327 ± 3[c]	1246	1320
6	e_{2g}	608	521	519	526
7	e_{2g}	3057	3077	3100	3092
8	e_{2g}	1600[d]	1516	1454	1521
9	e_{2g}	1178	1148	1147	1145
12	b_{1u}	1010		936	928
13	b_{1u}	3057[e]		3159	3167
14	b_{2u}	1310	1570	1567	1572
15	b_{2u}	1149	1150	1150	1148
18	e_{1u}	1038	920	921	930
19	e_{1u}	1484	1405 ± 3[c]	1407	1359
20	e_{1u}	3065[d]	3084 ± 5[cd]	3081	3061

[a] Reassignment from AP[23] value of 3130 cm^{-1}

[b] Deduced from analysis of combination bands in IR spectra

[c] This work

[d] Deperturbed value; mode is part of a Fermi resonance

[e] Estimated from isotopic product and sum rules

Table IIb. $\tilde{X}$ and $\tilde{A}$ state frequencies of out-of-plane modes.

(For footnotes see Table IIa)

Mode	Symmetry	Observed (cm^{-1})		Robey-Schlag[5]
		$\tilde{X}$	$\tilde{A}$	
4	b_{2g}	707[b]	365	365
5	b_{2g}	990[b]	745	750
10	e_{1g}	847	581	585
11	a_{2u}	674	515-518	514
16	e_{2u}	399	238	239
17	e_{2u}	967[b]	717	712

FIGURE CAPTIONS

Figure 1. Normal modes and their symmetries in benzene. Exact atomic displacements may be different in the $\tilde{X}$ and $\tilde{A}$ states.

Figure 2. (a) Two-photon (IR-UV double resonance) route to C-H stretches (CH^1) in the $\tilde{A}$ state. IR pumping populates the CH_1 state, and the CH_1^1 transition excites the CH^1 level. In this example the C-H stretching frequency is larger in the excited state: $\nu'_{CH} > \nu''_{CH}$. (b) Spectrum observed; IR is tuned to pump CH_1. The change in UV absorption vs. UV frequency with IR pumping turned on is sketched. The population in 0_0 is depleted and that in CH_1 is increased. The 0_0^0 transition probes the depletion, and the CH_1^1 transition is the double resonance which allows determination of ν'_{CH}.

Figure 3. Experimental apparatus which includes tunable IR (pump) and UV (probe) sources, a pulsed supersonic molecular beam of benzene seeded in argon, ion extraction and detection, and control electronics. The IR beam around 3000 cm^{-1} excites C-H stretches and is chopped with a beam flag. The UV laser frequency is scanned in order to find new $\tilde{A}$ state vibrational levels. Benzene UV transitions are detected with resonantly-enhanced two-photon ionization (R2PI.)

Figure 4. (a) Resonantly-enhanced two-photon ionization (R2PI) spectrum in the vicinity of the 6_1^0 band. (b) R2PI spectrum near the 6_0^1 band, which is extremely saturated in this scan. (c) Energy level diagram with vibrational angular momentum splitting and thermally excited levels. All transitions in this picture have $\Delta v_6 = \pm 1$.

Figure 5. Effect of vibrational angular momentum on UV transitions involving doubly-degenerate modes (e.g. ν_6). The vibrational angular momentum quantum number ℓ_i takes on the values v_i, $v_i - 2$, ... $-v_i$. For mode i, the energy shift due to vibrational angular momentum interactions is $g_{i,i}\ \ell_i^2$. The selection rule on ℓ during an optical transition in which $\Delta v = \pm 1$ is $\Delta\ell = \pm 1$. (a) Energy levels and allowed transitions of the different ℓ components. (b) Splitting of 4 g' observed in transitions from $\ell'' = 1$ states. In benzene, $g'_{6,6} = 1.7$ cm^{-1}, so the 6^2_1 splitting is ~ 7 cm^{-1}. The 6^1_0 and 6^0_1 transitions are not split.

Figure 6. IR spectrum of C-H stretching region, obtained with the UV laser tuned to 6^1_0. The 3101-cm^{-1} peak is an unresolved doublet. Our a", b", c" labeling of the peaks reflects the fact that zeroth-order names (ν''_{20}, $\nu''_8 + \nu''_{19}$, $\nu''_1 + \nu''_6 + \nu''_{19}$) are inappropriate because of mode mixing.

Figure 7. Energy level diagram of the C-H stretching Fermi triad. The traditional assignment of each observed level (a",b",c") is written above the level corresponding to its zeroth-order "parent".

Figure 8. (a) UV transitions beginning from mixed, IR-pumped levels. No transitions are forbidden, because the ground-state vibrational levels are mixed differently from the excited-state ones. As the heavy lines show, the most intense transitions are those which retain the ground-state vibrational "character." (b) Double-resonance spectra aligned with respect to total (IR + UV) energy. Transitions to common

final states are vertically aligned. Only peaks are shown; in general, dips (see Fig. 1b) are present also. Frequencies of modes 3, 19, and 20 are deduced from these spectra, as is the presence of the $3_1 6_1 15_1$ state in the c" level.

Figure 9. Double resonance spectra around 6^0_1. Dips in the spectra (e.g. 6_1) are assigned according to the ground-state population that caused them. Labels next to peaks are our assignments of the final vibrational states. Frequencies of modes 3, 19, and 20 are deduced from these spectra, as is the presence of the $3_1 6_1 15_1$ state in the c" level.

Figure 10. As in Figure 9, for the 6^1_0 region.

Figure 11. Upper states in double resonance transitions. The selection rules $\Delta v_6 = \pm 1$, Δv_1 = anything, have been used to find the final states accessible in the 6^0_1 region, and the 6^1_0 region. The lower states are a", b", and c" (the mixed 20_1, $8_1 19_1$, and $1_1 6_1 19_1$ levels). In this figure, the heavy lines show the most intense transitions. Those with $v_1' = v_1'' = 1$ have small Franck-Condon factors, and are shown with fainter lines. Levels with $v_2' = 2$ or $v_6' = v_8' = 1$ have a vibrational angular momentum splitting, producing a doublet. The $1^1 6^2 19^1$ level, shown with dashed lines, is outside the energy range we scanned. The $6^2 19^1$ and $1^1 19^1$ levels are separated by $2\nu_6' - \nu_1' \approx 120$ cm^{-1}. Likewise, the $6^1 8^1 19^1$ level is $\nu_8' - \nu_6' \approx 995$ cm^{-1} above the $6^2 19^1$ level.

Figure 12. Benzene C-H stretching Fermi tetrad, according to Pliva's analysis and confirmed by us. $\nu_3'' + \nu_6'' + \nu_{15}''$ is only mixed into the 3101-cm^{-1} level, and $\nu_1'' + \nu_6'' + \nu_{19}''$ is now in the middle.

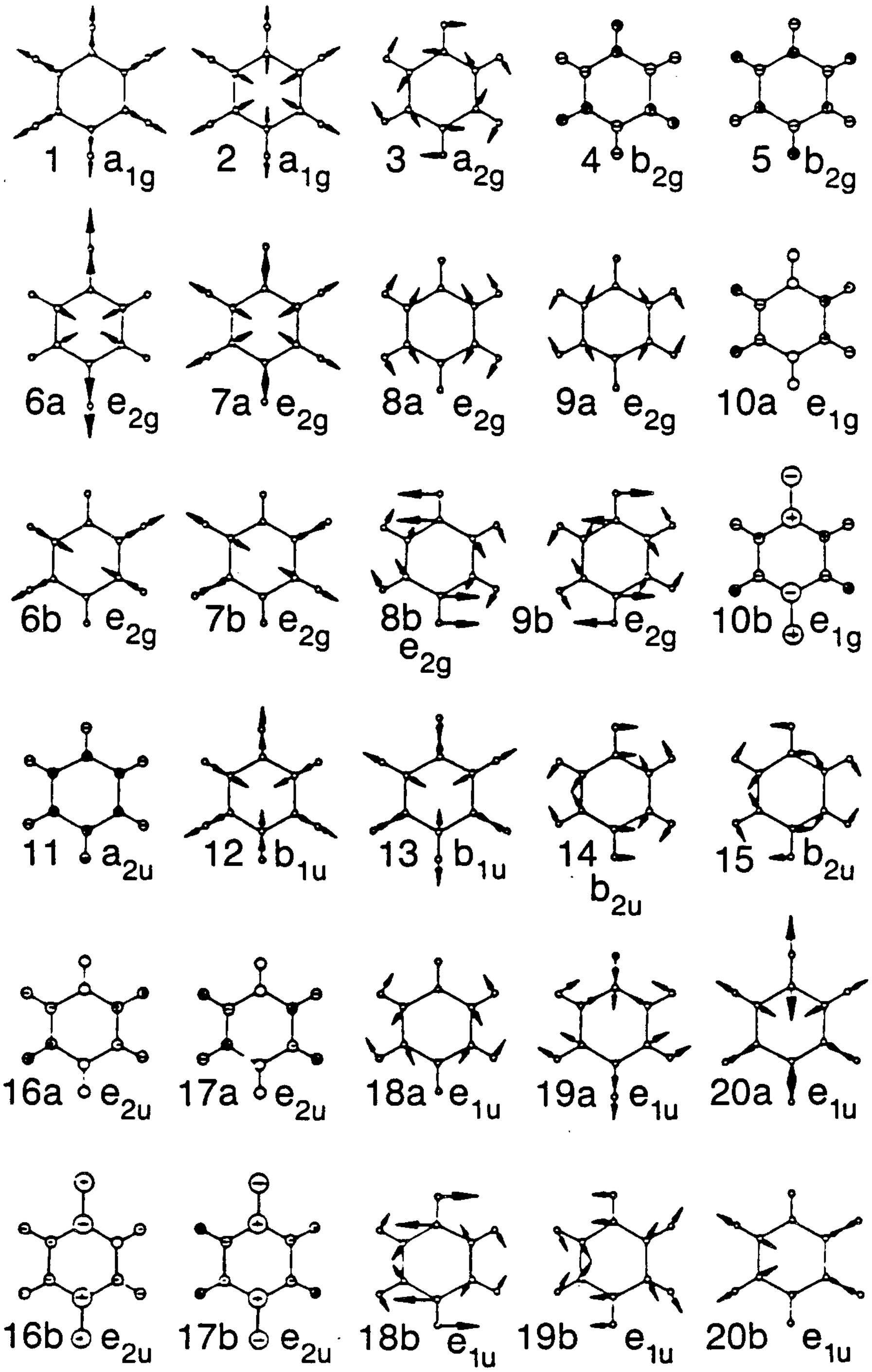

Normal modes of Benzene (Wilson's numbering)

XBL 872-6153

IR-UV double resonance

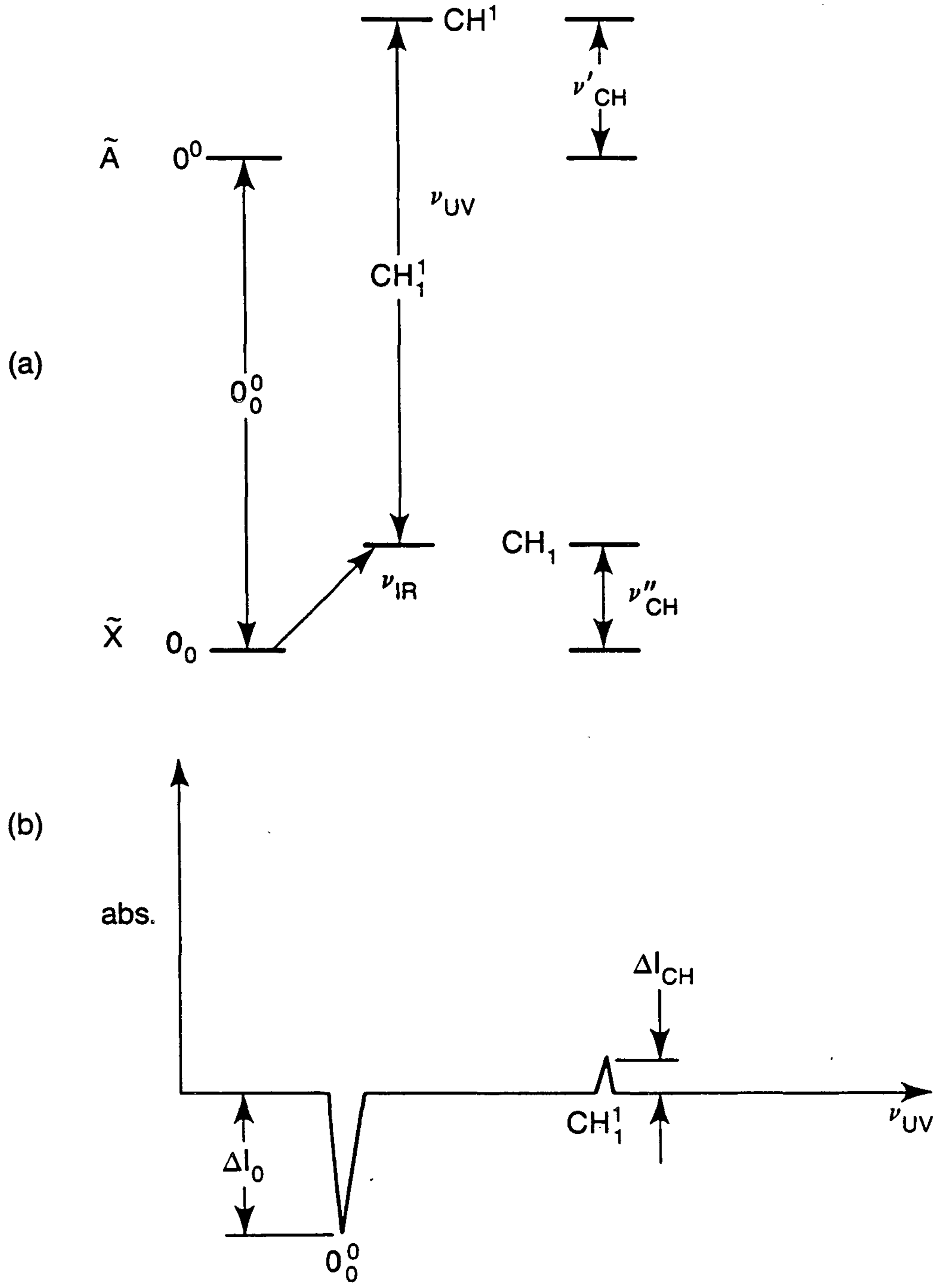

XBL-872-6190

Experimental apparatus for obtaining IR-UV double resonance spectra

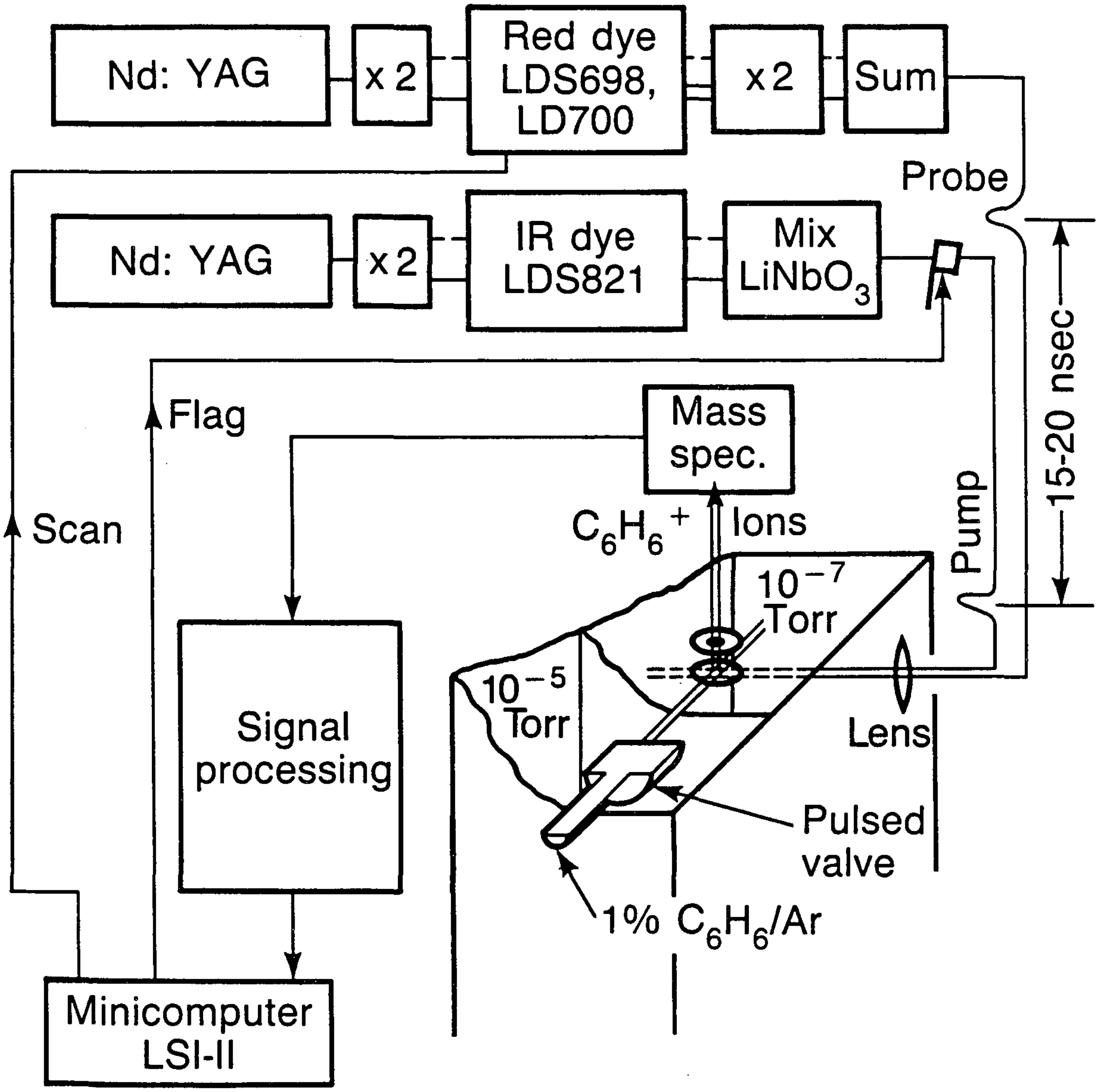

XBL 872-6183

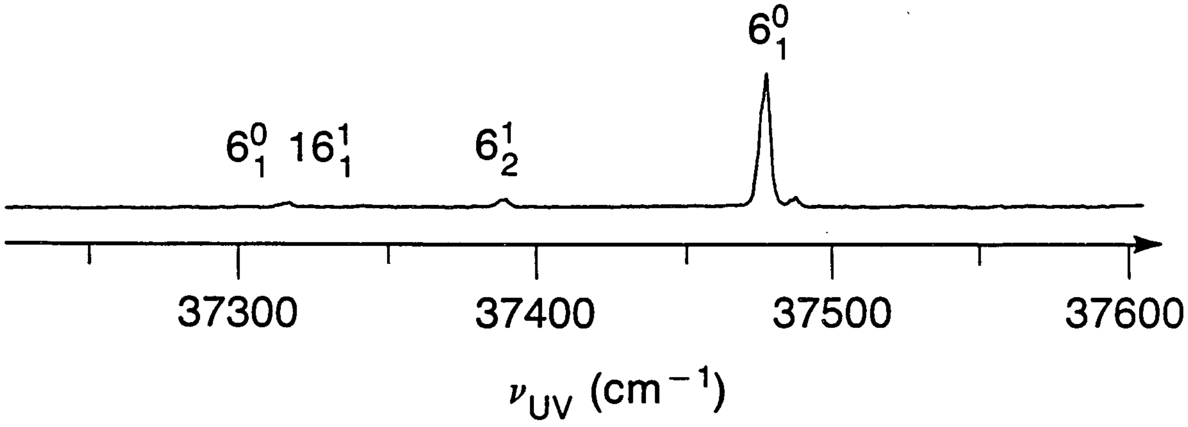

R2PI spectrum around 6^0_1

XBL 872-6176

R2PI spectrum around 6^1_0

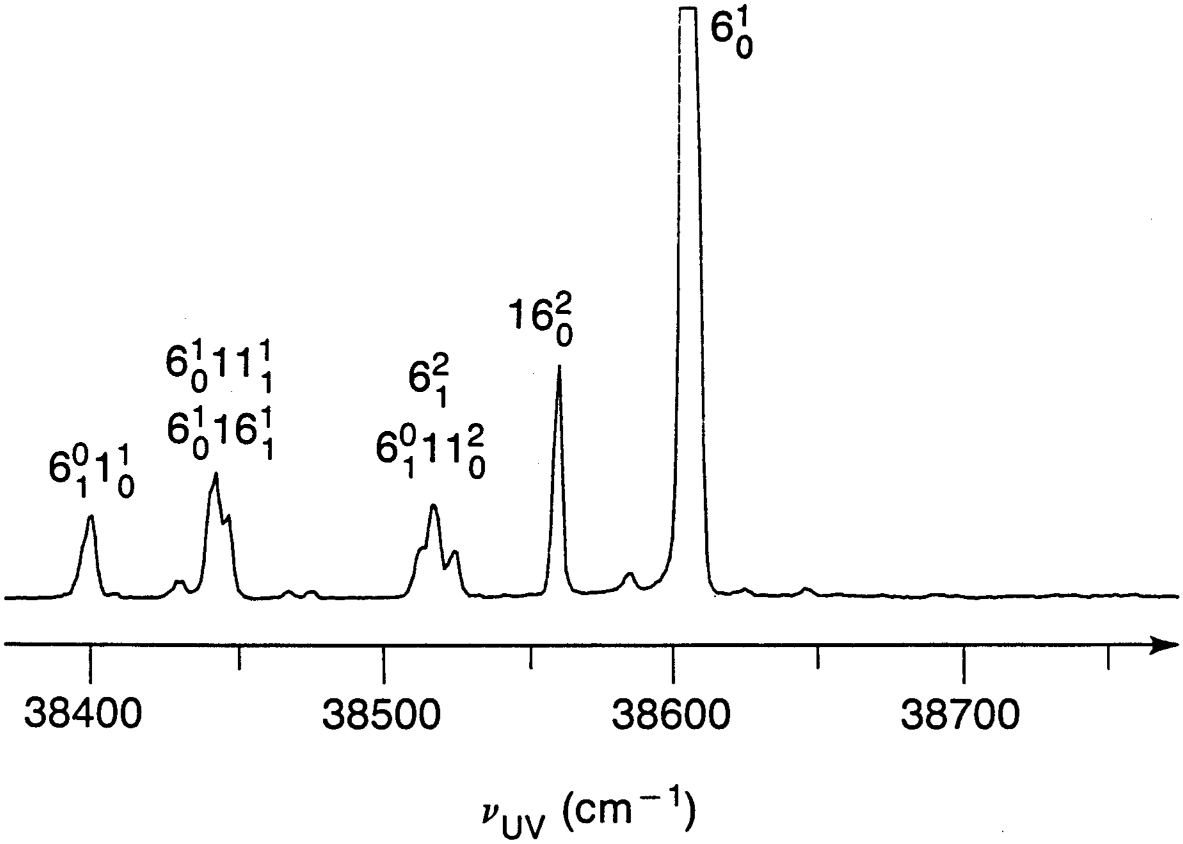

XBL 872-6175

Benzene energy levels and UV transitions

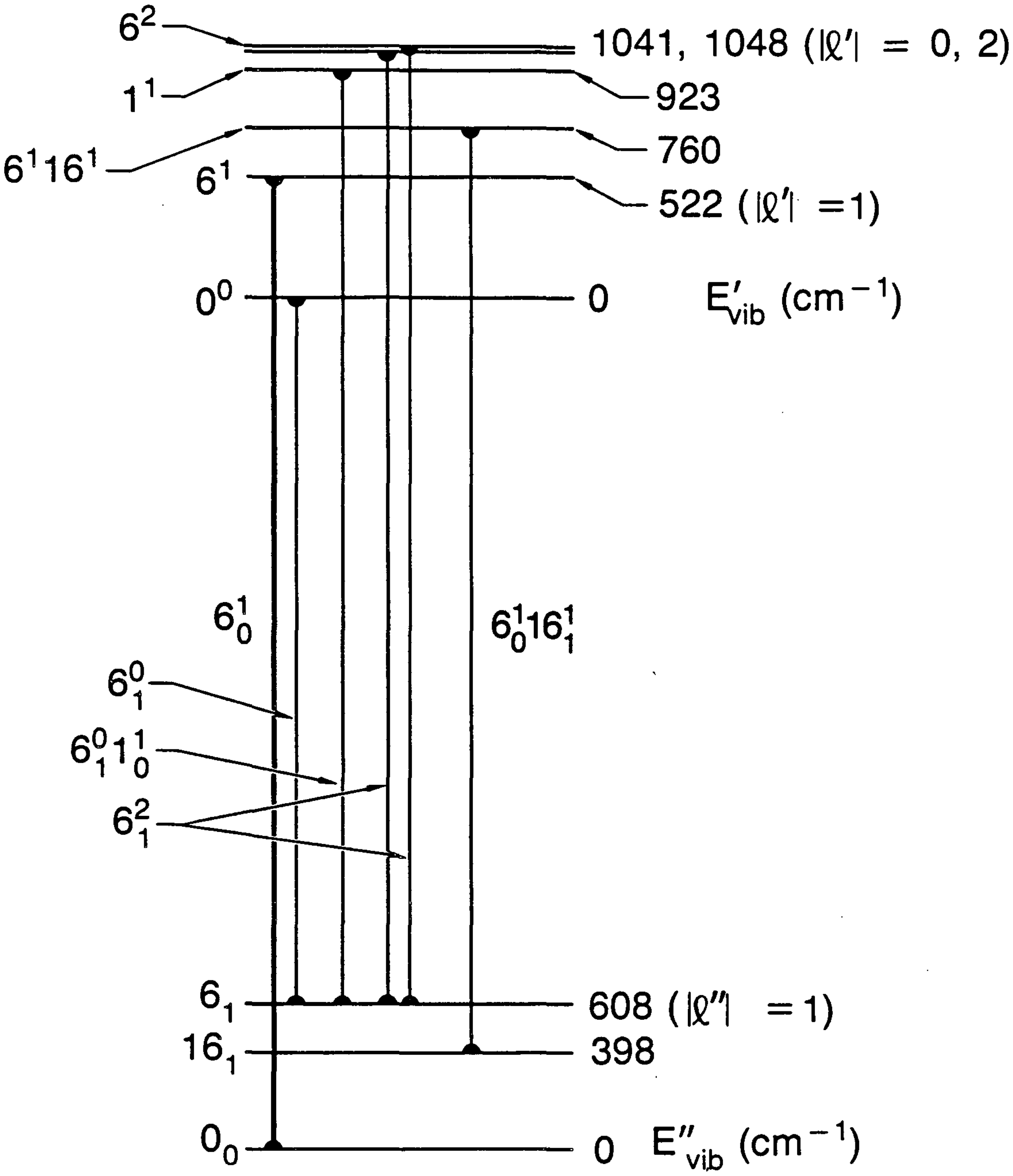

XBL 872-6119

Vibrational angular momentum selection rules and splittings

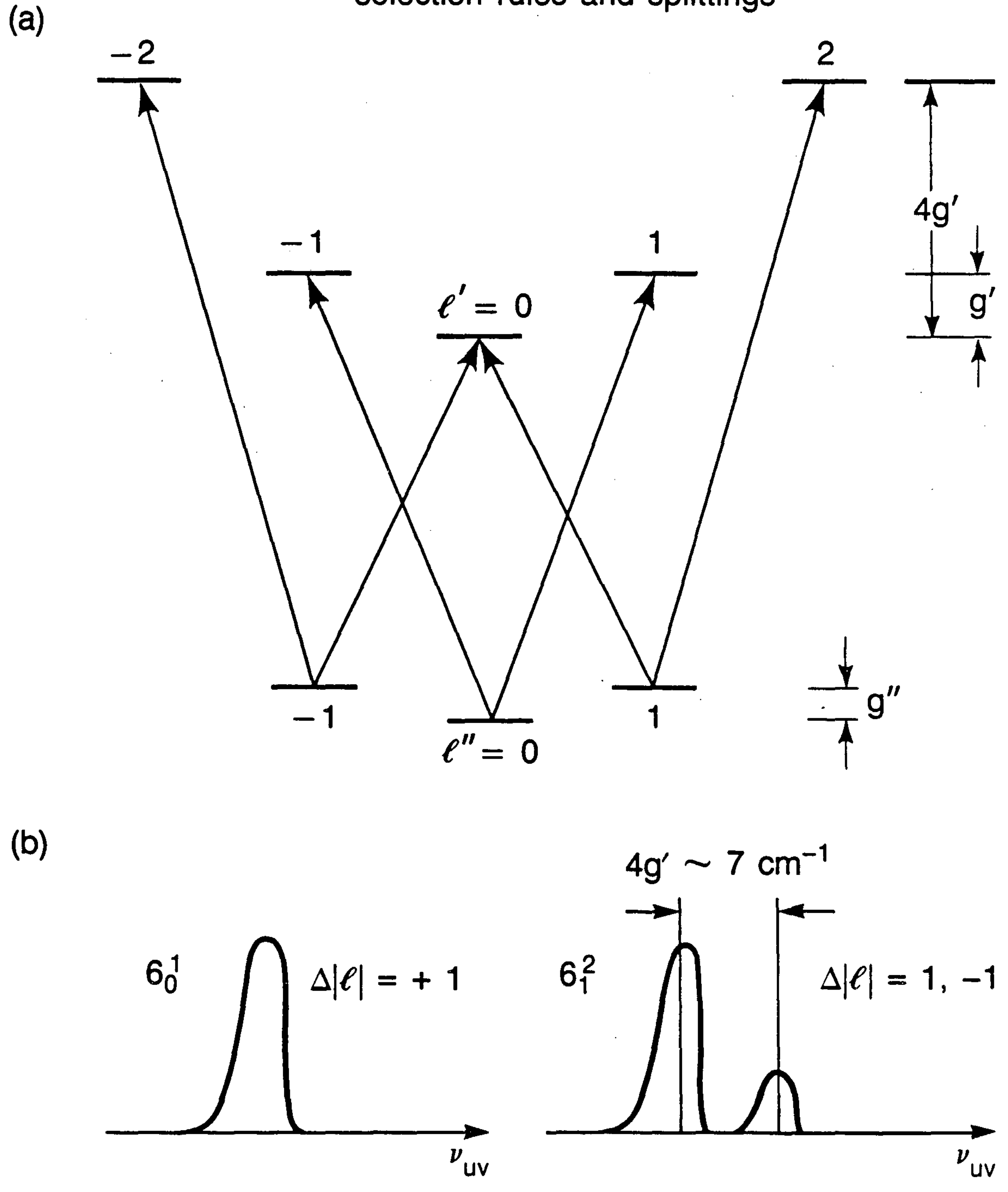

XBL-872-6118

Spectrum of C-H Stretching "Fermi triad"

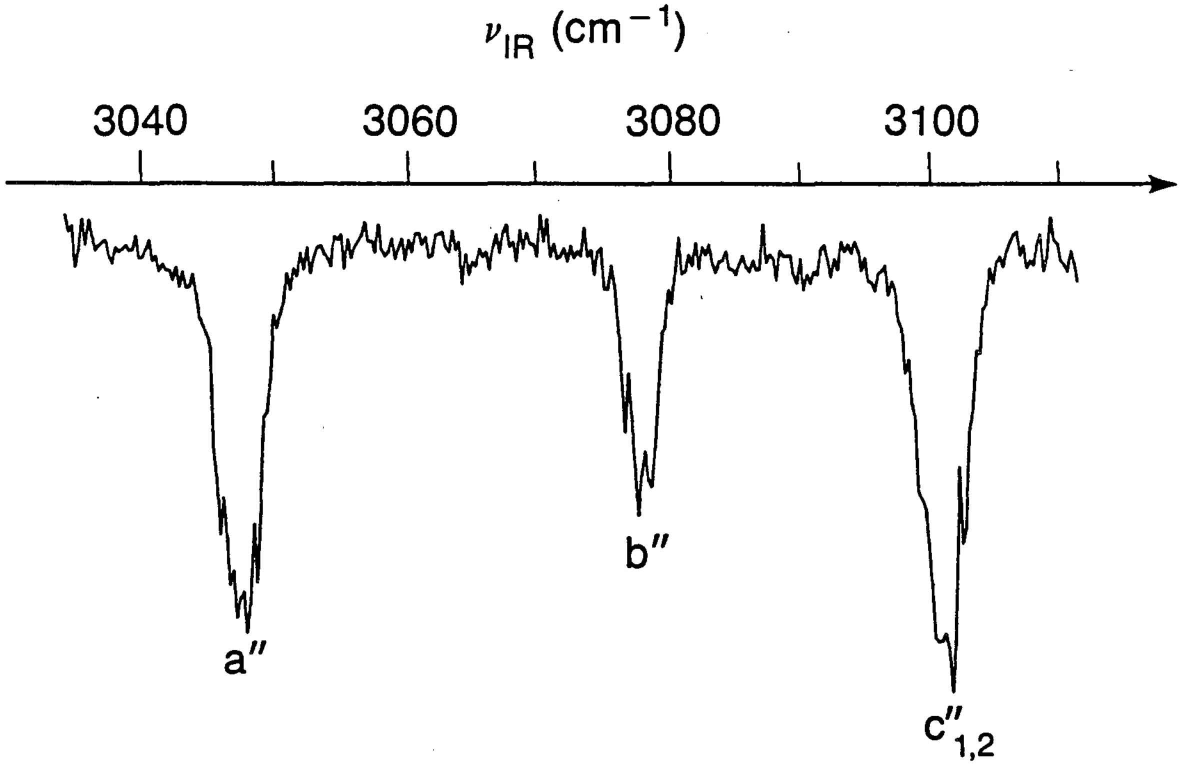

XBL 872-6157

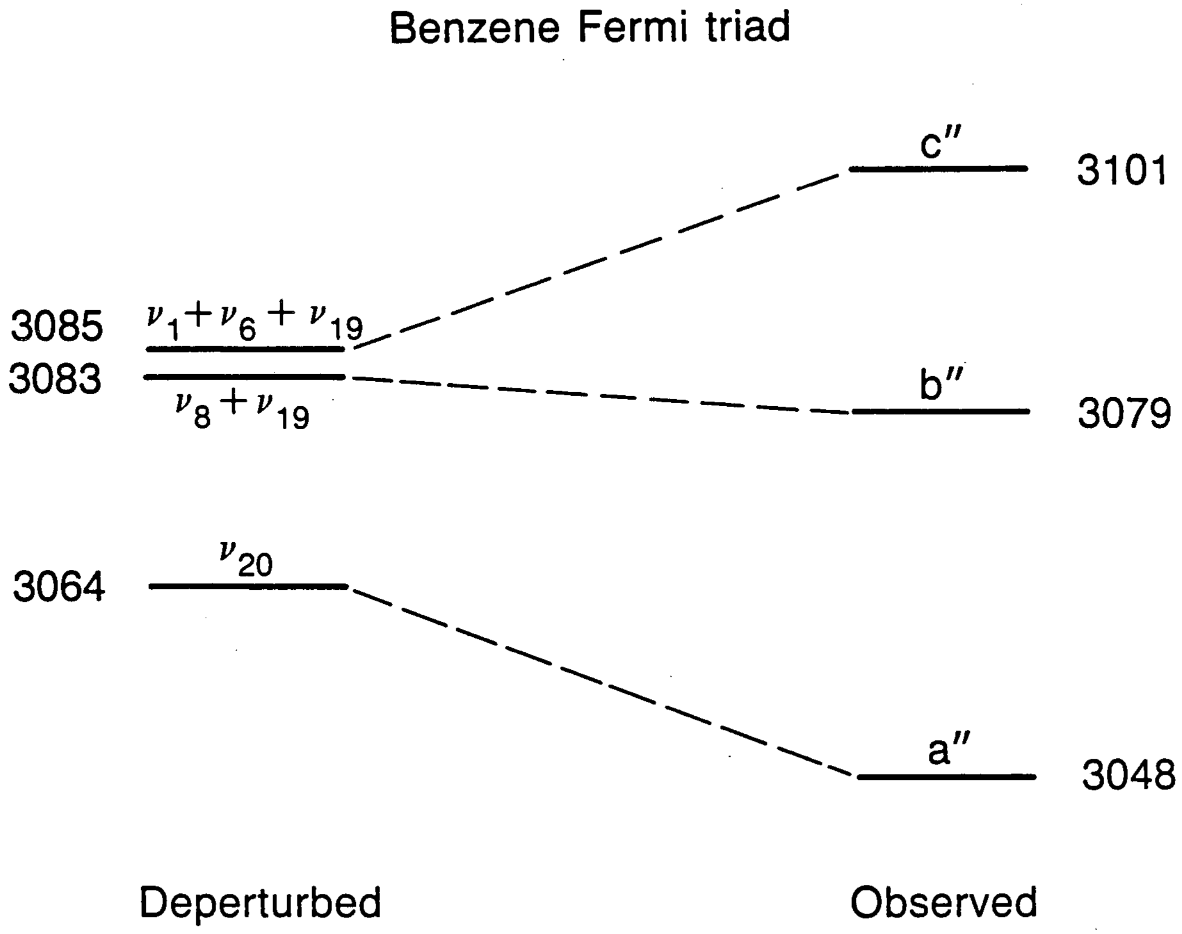
Benzene Fermi triad
3085
$\nu_1 + \nu_6 + \nu_{19}$
3083
$\nu_8 + \nu_{19}$
3064
ν_{20}
c″
3101
b″
3079
a″
3048
Deperturbed
Observed

XBL 872-6191

Allowed transitions from mixed levels

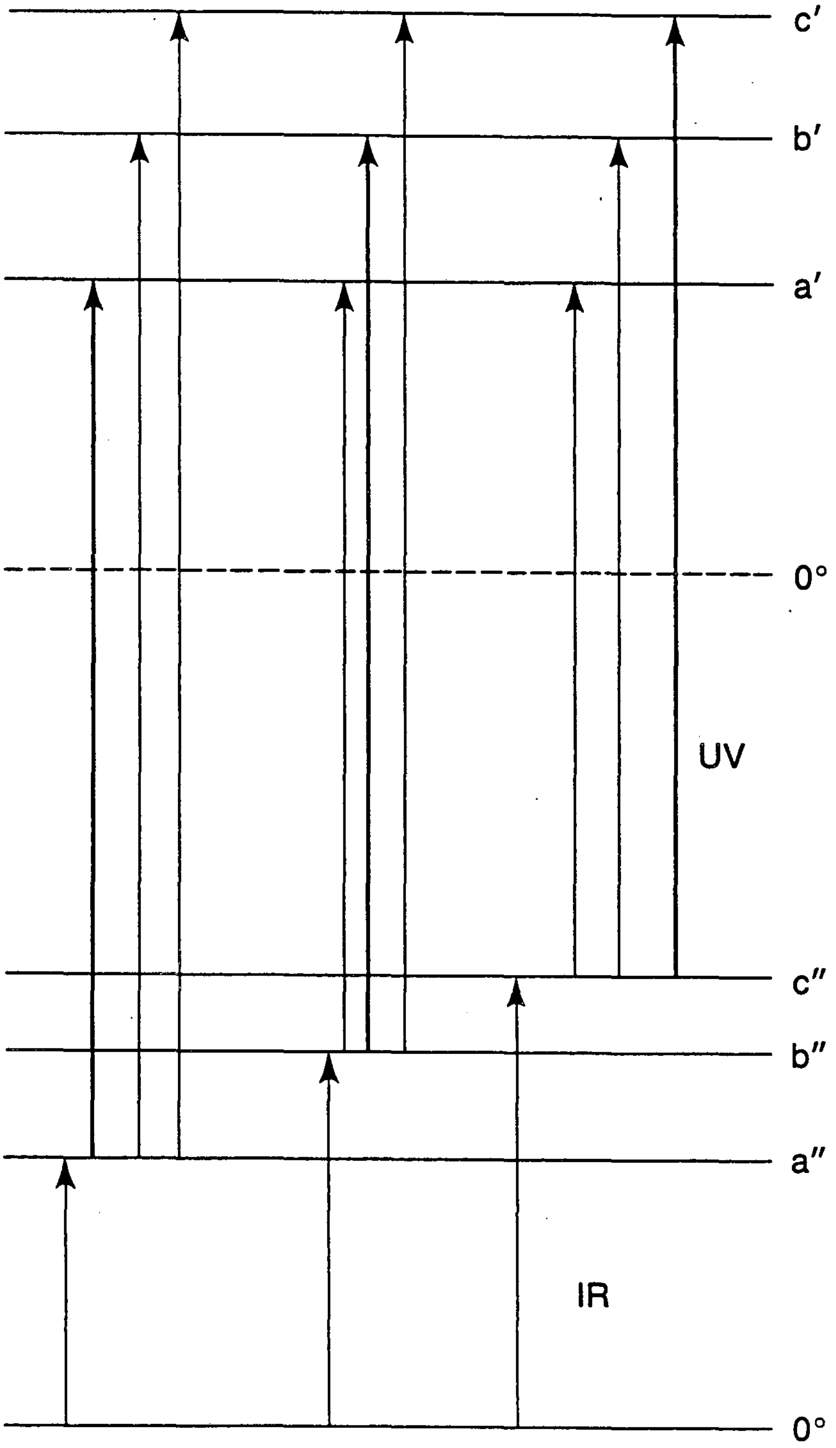

XBL-872-6182

Resulting UV spectra with IR fixed on a″ — c″

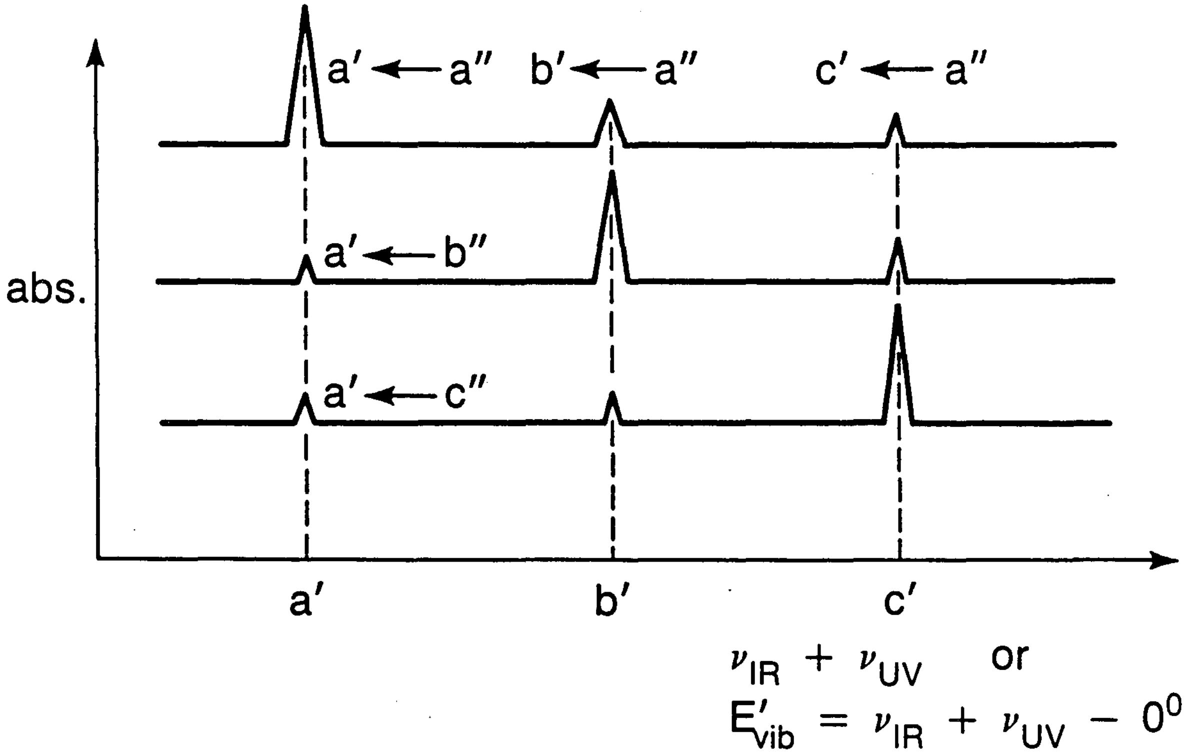

XBL 872-6180

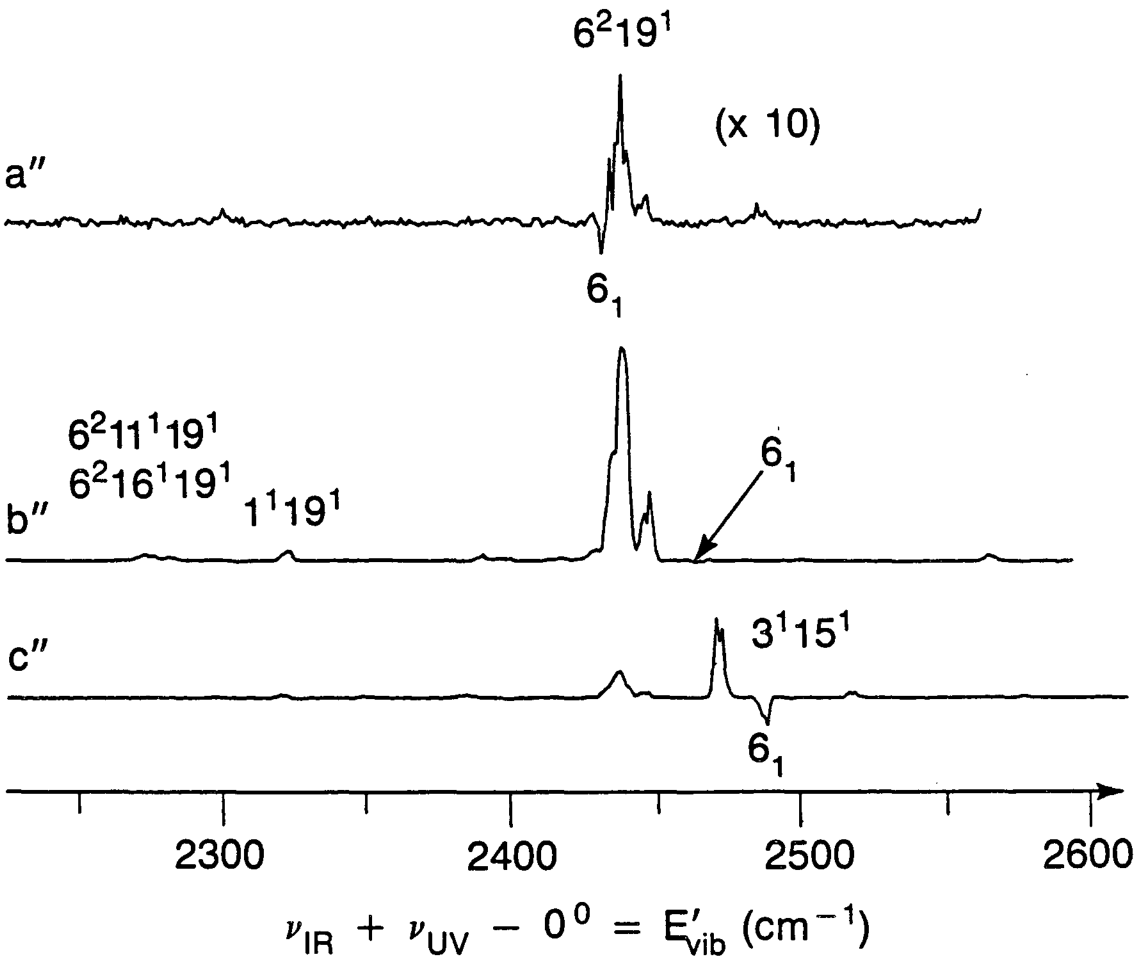

Double resonance spectra around 6^0_1

XBL 872-6155

Double resonance spectra around 6^1_0

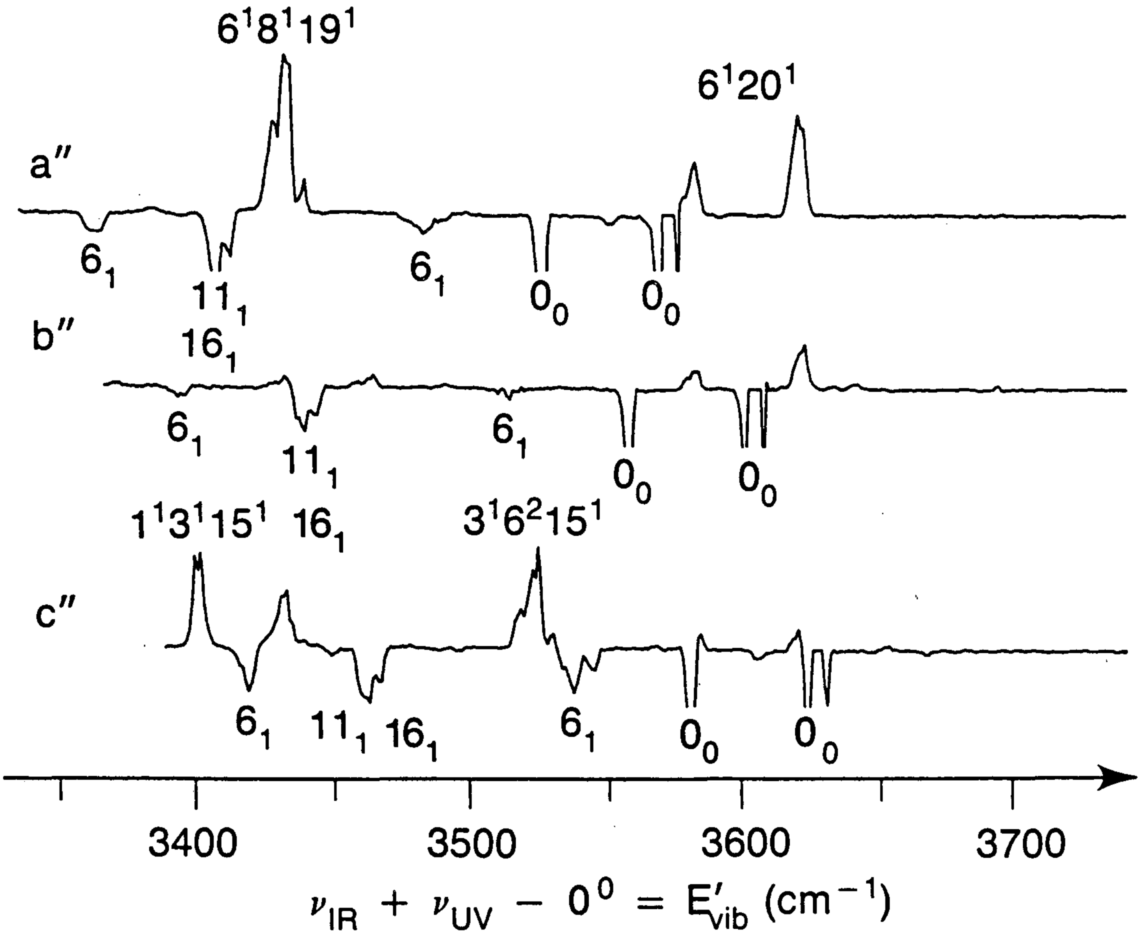

XBL 872-6156

Upper States in Double Resonance Transitions

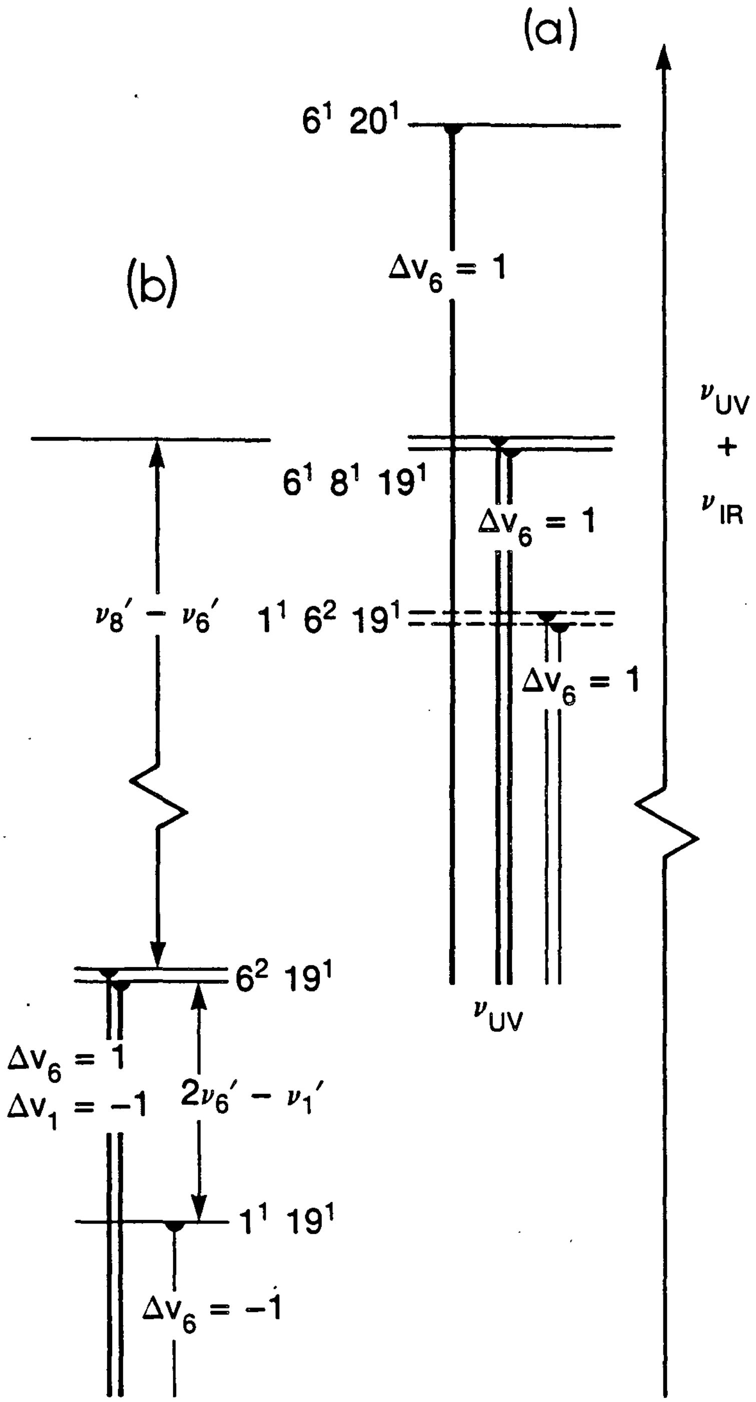

XBL 874-7668

Benzene Fermi tetrad

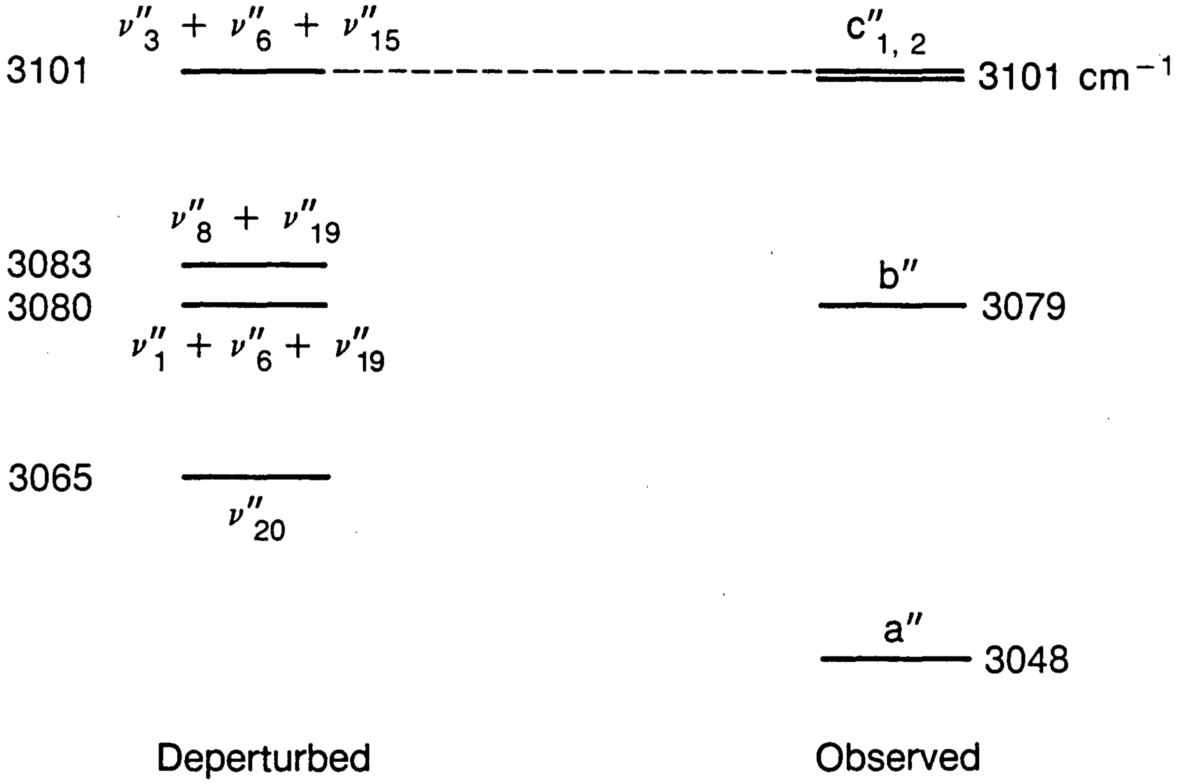

XBL 872-6179

LAWRENCE BERKELEY LABORATORY
TECHNICAL INFORMATION DEPARTMENT
UNIVERSITY OF CALIFORNIA
BERKELEY, CALIFORNIA 94720